AEDC-TSR-90-V13

(2)

AD-A228 231

INVESTIGATION OF THE INFLUENCE OF CONSTANT ADVERSE PRESSURE GRADIENTS ON LAMINAR BOUNDARY-LAYER STABILITY AT MACH NUMBER 8

J. C. Donaldson, J. P. Grubb, and D. W. Sinclair
Calspan Corporation/AEDC Operations

October 1990

Final Report for May 7-11, 1990

Approved for public release; distribution is unlimited.

ARNOLD ENGINEERING DEVELOPMENT CENTER
ARNOLD AIR FORCE BASE, TENNESSEE
AIR FORCE SYSTEMS COMMAND
UNITED STATES AIR FORCE

APPROVAL STATEMENT

This report has been reviewed and approved.

Richard Rushing

RICHARD RUSHING
Reentry Systems Division
Dir of Aerospace Flt Dyn Test
Deputy for Operations

Approved for publication:

FOR THE COMMANDER

Ray B. Williamson

RAY B. WILLIAMSON, Maj, USAF
Chief, Reentry Systems Division
Dir of Aerospace Flt Dyn Test
Deputy for Operations

REPORT DOCUMENTATION PAGE

Form Approved
OMB No. 0704-0188

1. AGENCY USE ONLY (Leave blank)	2. REPORT DATE	3. REPORT TYPE AND DATES COVERED
	October 1990	Final Report for May 7-11, 1990

4. TITLE AND SUBTITLE
Investigation of the Influence of Constant Adverse Pressure Gradients on Laminar Boundary-Layer Stability at Mach Number 8

5. FUNDING NUMBERS
PE 61102F

6. AUTHOR(S)
Donaldson, J. C., Grubb, J. P., and Sinclair, D. W., Calspan Corporation/AEDC Operations

7. PERFORMING ORGANIZATION NAME(S) AND ADDRESS(ES)
Arnold Engineering Development Center/DOF
Air Force Systems Command
Arnold Air Force Base, TN 37389-5000

8. PERFORMING ORGANIZATION REPORT NUMBER
AEDC-TSR-90-V13

9. SPONSORING/MONITORING AGENCY NAMES(S) AND ADDRESS(ES)
WRDC/FIMG
Wright-Patterson AFB, OH 45433

10. SPONSORING/MONITORING AGENCY REPORT NUMBER

11. SUPPLEMENTARY NOTES
Available in Defense Technical Information Center (DTIC).

12a. DISTRIBUTION/AVAILABILITY STATEMENT
Approved for public release; distribution is unlimited.

12b. DISTRIBUTION CODE

13. ABSTRACT (Maximum 200 words)
Measurements of fluctuating-flow and mean-flow parameters were made in the boundary layer on each of two axisymmetric, constant pressure gradient bodies in an investigation of the influence of adverse pressure gradients on the stability of a laminar boundary layer in hypersonic flow. Each test article was a slender, constant pressure gradient flare combined with a sharp cone forebody with a 7-deg half angle. The test articles differed in the magnitude of the pressure gradient. The flow-fluctuation measurements were made using constant-current hot-wire anemometry techniques. Boundary-layer profiles and model surface conditions were measured to supplement the hot-wire data. Testing was done at Mach number 8 with a free-stream unit Reynolds number of 1.0-million per foot. The test equipment, test techniques, and the data acquisition and reduction procedures are described. Analysis of the hot-wire anemometer data is beyond the scope of this report. The test was the nineth in a series of efforts which have investigated various aspects of hypersonic boundary-layer stability.

14. SUBJECT TERMS
hypersonic flow; boundary-layer stability.
wind tunnel ~~flow~~; hot-wire anemometry
adverse pressure gradients; sharp cone with flare

15. NUMBER OF PAGES
59

16. PRICE CODE

17. SECURITY CLASSIFICATION OF REPORT	18. SECURITY CLASSIFICATION OF THIS PAGE	19. SECURITY CLASSIFICATION OF ABSTRACT	20. LIMITATION OF ABSTRACT
UNCLASSIFIED	UNCLASSIFIED	UNCLASSIFIED	SAME AS REPORT

COMPUTER GENERATED

Standard Form 298 (Rev. 2-89)
Prescribed by ANSI Std. Z39-18
298-102

CONTENTS

ILLUSTRATIONS

Figures

TABLES

SAMPLE DATA

NOMENCLATURE

ALPHA	Angle of attack, deg
CONFIG	Model configuration designation
CP	Pressure coefficient, (PW-P)/Q
CPC	Pressure coefficient on forecone
CSF	Schmidt-Boelter gage calibration factor, Btu/ft^2 - sec - mv
CURRENT	Hot-wire or hot-film anemometer heating current, mamp
D	Diameter of thermocouple junction of total temperature probe, in.
DATA TYPE	Code indicating nature of data tabulated:
	"2" - Model surface pressure and temperature measurements
	"4" - Mean boundary-layer profile measurements using pitot pressure and total temperature probes
	"6" - Probe calibration measurements in free stream
	"9" - Hot-wire and hot-film anemometer probe measurements
DCPX	Gradient of pressure coefficient, dCP/dX, in.$^{-1}$
DEL	Boundary-layer total thickness, in.
DEL*	Boundary-layer displacement thickness, in.
DEL**	Boundary-layer momentum thickness, in.
DEW	Tunnel stilling chamber dew point temperature, °F
DITTD	Enthalpy difference at boundary-layer thickness, DEL, ITTD-ITWL, Btu/lbm
DITTL	Local enthalpy difference, ITTL-ITWL, Btu/lbm
E	Schmidt-Boelter gage output, mv
EBAR	Hot-wire or hot-film anemometer mean voltage, mv

ERMSA	Amplified hot-wire anemometer output rms voltage, mv rms
ERMSF	Amplified hot-film anemometer output rms voltage, mv rms
ETA	Effective total-temperature probe recovery factor ETA=(TTLU-T)/(TT-T) or (TTTU-T)/(TT-T)
FIL	Identification of data file used for plot
GAGE	Identification for Schmidt-Boelter gage
H (TT), HT (TT)	Heat-transfer coefficient based on TT, QDOT/(TT-TW), Btu/ft^2-sec-°R
ITT	Enthalpy based on TT, Btu/lbm
ITTD	Enthalpy based on TTD, Btu/lbm
ITTL	Enthalpy based on TTL, Btu/lbm
ITW	Enthalpy based on TW, Btu/lbm
ITWL	Enthalpy based on TWL, Btu/lbm
K	Schmidt-Boelter gage temperature calibration factor, °F/mv
L	Total model length, in.
LRE	Local unit Reynolds number, in.$^{-1}$
LRED	Unit Reynolds number at the boundary-layer thickness, DEL, in.$^{-1}$
LRET	Local "normal shock" unit Reynolds number (based on MUTTL), in.$^{-1}$
LRETD	"Normal shock" unit Reynolds number at boundary-layer thickness, DEL, (based on MUTTD), in.$^{-1}$
M, MACH	Free-stream Mach number
MD	Local Mach number at boundary-layer thickness, DEL
ME	Mach number at boundary-layer edge
ML	Local Mach number
MS	Model station, in.
MU	Dynamic viscosity based on T, lbf-sec/ft^2

MUTD	Dynamic viscosity based on TD, lbf-sec/ft^2
MUTL	Dynamic viscosity based on TL, lbf-sec/ft^2
MUTT	Dynamic viscosity based on TT, lbf-sec/ft^2
MUTTD	Dynamic viscosity based on TTD, lbf-sec/ft^2
MUTTL	Dynamic viscosity based on TTL, lbf-sec/ft^2
P	Free-stream static pressure, psia
PHI	Roll angle, deg
POINT	Data point number
PP	Pitot probe pressure, psia
PPD	Pitot pressure at boundary-layer thickness, DEL, psia
PPE	Pitot pressure at boundary-layer edge, psia
PT	Tunnel stilling chamber pressure, psia
PT2	Free-stream total pressure downstream of a normal shock wave, psia
PW	Model surface pressure, psia
PWL	Model wall static pressure used for boundary-layer survey calculations, psia
Q	Free-stream dynamic pressure, psia
QDOT	Heat-transfer rate, Btu/ft^2-sec
RE, RE/FT	Free-stream unit Reynolds number, in.$^{-1}$ or ft^{-1}
RETD	Free-stream "normal shock" Reynolds number (based on MUTT and D)
RHO	Free-stream density, lbm/ft^3
RHOD, RHD	Density at boundary-layer thickness, DEL, lbm/ft^3
RHOL, RHL	Local density, lbm/ft^3
RHOUD	(RHOD) * (UD), lbm/sec-ft^2
RN	Model nose radius, in.
RUN	Data set identification number

RX	Local radius of model at X, in.
SET	Identification of probe assembly
ST(TT)	Stanton number based on stilling chamber temperature (TT), $ST(TT) = \frac{QDOT}{(RHO)\ (V)(ITT-ITW)}$
T	Free-stream static temperature, °R, or °F
ΔT	Temperature difference, °F
TAP	Pressure orifice identification number
T/C	Identification for model surface temperature measured by Schmidt-Boelter gage thermocouple
TD	Static temperature at boundary-layer thickness, DEL, °R
TDRK	Temperature of Druck probe transducer, °F
TG	Schmidt-Boelter gage embedded thermocouple temperature, °R
THETA	Peripheral angle on the model measured from ray on model top, positive clockwise when looking downstream, deg
THTC	Forecone half angle, deg
TL	Local static temperature, °R
TT	Tunnel stilling chamber temperature, °R, or °F
TTD	Total temperature at boundary-layer thickness, DEL, °R
TTE	Total temperature at boundary-layer edge, °R
TTL	Local total temperature, °R
TTLU	Uncorrected (measured) probe recovery temperature interpolated at the pitot probe location, ZP, °R
TTTU	Uncorrected (measured) probe recovery temperature at ZT, °R
TW	Schmidt-Boelter gage surface temperature, °R
TWL	Model wall temperature used for boundary-layer survey calculations, °R

UD	Local velocity component parallel to model surface at boundary-layer thickness, DEL, ft/sec
UE	Local velocity component parallel to model surface at boundary-layer edge, ft/sec
UL	Local velocity component parallel to model surface, ft/sec
V	Free-stream velocity, ft/sec
VF	Exponent for power-law flare body
X	Axial location measured from virtual apex of model, in.
XC	Calculated X location of survey station, in.
XJ	Nominal X location of cone-flare junction, in.
XSTA	Nominal X location of survey station, in.
ZA	Hot-wire anemometer probe height, distance to probe centerline along normal to model surface, in.
ZF	Hot-film anemometer probe height, distance to probe centerline along normal to model surface, in.
ZP	Pitot-pressure probe height, distance to probe centerline along normal to model surface, in.
ZT	Total-temperature probe height, distance to probe centerline along normal to model surface, in.

1.0 INTRODUCTION

The work reported herein was conducted by the Arnold Engineering Development Center (AEDC), Air Force Systems Command (AFSC), under Program Element 61102F, Control Number 2307, at the request of the Wright Research and Development Center (WRDC/FIMG), Wright-Patterson Air Force Base, Ohio 45433-6553. The WRDC/FIMG project manager was Kenneth F. Stetson. The test results were obtained by the Calspan Corporation, operating contractor for the Aerospace Flight Dynamics testing effort at the AEDC, AFSC, Arnold Air Force Base, Tennessee. The test was conducted in the Hypersonic Wind Tunnel B of the von Karman Gas Dynamics Facility during the period from May 7 to 11, 1990, under AEDC Project Number CP91VB (Tests Number 320 and 326).

The objective of this test was to investigate the influence of constant adverse pressure gradients upon the development of laminar boundary-layer flow instabilities in hypersonic flow. The test was the ninth in a series of cooperative efforts between WRDC/FIMG and AEDC/DOF which have investigated various aspects of hypersonic boundary-layer stability. The first seven tests examined the flow over sharp and blunt cones while the eighth test examined the flow over a hollow cylinder. Representative documentation of the previous tests is given in Refs. 1-5. Selected results of the tests involving the flow over cones are presented in Refs. 6-10.

Two axisymmetric models were designed and fabricated for this test. The two configurations had the same conical forebody and differed in the value of the design pressure gradient of the flare afterbody. The principal measurements of this investigation were hot-wire anemometer probe data acquired at the position in the local boundary-layer profile where the disturbance energy, sensed by the anemometer probe, was maximum. These data were obtained at 27 stations located at one-inch intervals of X along each of the models. Additional anemometer data were acquired, using hot-film probes, to evaluate the capabilities of the film probe for tests of this nature. The anemometer data were supplemented by surveys of the boundary layer on each model using pitot pressure and total temperature probes. Measurements of model surface pressure, temperature, and heat-flux were also made on both models. The testing was done at free-stream Mach number 8, generally at a free-stream unit Reynolds number of one-million per foot, at nominal zero angle of attack. A limited amount of model surface data was obtained at additional unit Reynolds numbers.

The purpose of this report is to document the test and to describe the test parameters. The report provides information to permit use of the data but does not include any data analysis, which is beyond the scope of the report.

The final data from the test have been transmitted to WRDC/FIMG. Requests for the data should be addressed to WRDC/FIMG, Wright-Patterson Air Force Base, Ohio 45433-6553. A copy of the data is on file at the AEDC.

2.0 APPARATUS

2.1 TEST FACILITY

The AEDC Hypersonic Wind Tunnel B (Fig. 1) is a closed-circuit wind tunnel with a 50-in.-diameter test section. Two axisymmetric contoured nozzles are available to provide Mach numbers of 6 and 8, and the tunnel may be operated continuously over a range of pressure from 40 to 300 psia at Mach number 6, and 100 to 900 psia at Mach number 8, with air supplied by the von Karman Gas Dynamics Facility (VKF) main compressor plant. Stagnation temperatures sufficient to avoid air liquefaction in the test section (up to 1,350°R) are obtained through the use of a natural gas fired combustion heater. The entire tunnel (throat, nozzle, test section, and diffuser) is cooled by integral, external water jackets. The tunnel is equipped with a model injection system, which allows removal of the model from the test section while the tunnel remains in operation. A description of the tunnel and airflow calibration information may be found in Ref. 11.

2.2 TEST ARTICLES

Two axisymmetric test articles (Fig. 2), fabricated of type 17-4 PH stainless steel, were supplied for this investigation by WRDC/FIMG. Each model had a total axial length of 40 in., and the contour was divided into three sections: (1) a conical forebody (19 in. long) with a sharp nose and 7-deg vertex half angle, (2) a quintic fillet (3 in. long) which provided continuous curvature between the forecone and the after body, and (3) a slender constant adverse pressure gradient flare (18 in. long). The two models differed in the value of the design pressure gradient. The contour of each model was developed by AEDC under another project for WRDC using modified Newtonian theory. The contour was partially validated with inviscid computational fluid dynamic calculations by AEDC. The design Mach number was 8. The resulting theoretical flare was a power-law body. For the lower value of design pressure gradient, a power-law exponent of 1.50 provided an adequate constant pressure gradient distribution with $d(PW/P)/dX = 0.04$ per in., nominal. This model, with the smaller pressure gradient, was designated DP/DX:1. For the larger-gradient flare, the exponent was relaxed to a value of 1.43 to improve the flatness of the theoretical gradient distribution with $d(PW/P)/dX = 0.125$ per in., approximately. The model with the larger pressure gradient was designated DP/DX:4. The body geometry for the flare section was described by the equation

$$\frac{RX}{L} = \frac{\tan(THTC)}{L}\left[XJ + \frac{1}{(VF)}\,\frac{(CPC)}{(DCPX)}\right]\left[\left(\frac{(L)\,(DCPX)}{(CPC)}\left(\frac{X}{L} - \frac{XJ}{L}\right) + 1\right)^{VF} - 1\right] \quad (1)$$

The test articles were mounted on the model injection system using a water-cooled sting. A photograph of the test installation of Configuration DP/DX:4 is shown in Fig. 3.

Each model was instrumented with 24 static pressure orifices: 21 orifices along the 180-deg (bottom) ray of the model and one orifice on each of the 0-, 90-, and 270-deg rays at X = 38 in. Each orifice was located in a plug press-fitted into the model surface, and the orifice diameter was 0.040 in. The stainless steel tubing connected to each orifice had an O.D. of 0.094 in. and an I.D. of 0.062 in. The smaller-gradient model was instrumented with 20 Schmidt-Boelter heat-transfer gages of 0.1875-in. diameter along the 90-deg ray of the model. The larger-gradient model was instrumented similarly but had seven additional gages between X = 36 and X = 38 in. along other rays. The locations of the orifices and gages are listed in Table 1 for both model configurations.

2.3 FLOW-FIELD SURVEY MECHANISM

Surveys of the flow field were made using a retractable survey system (X-Z Survey Mechanism) designed and fabricated by the AEDC. This mechanism makes it possible to change survey probes while the tunnel remains in operation. The mechanism is housed in an air lock immediately above a port in the top of the Tunnel B test section. Access to the test section is through a 40-in.-long by 4-in.-wide opening which is sealed by a pneumatically operated door when the mechanism is retracted. Separate drive motors are provided to (1) insert the mechanism into the test section or retract it into the housing (Z drive), (2) position the mechanism at any desired axial station over a range of 35 in. (X drive), and (3) survey a flow field of approximately 10-in. depth (Z' drive). A pneumatically operated shield is provided to protect the probes during injection and retraction through the tunnel boundary layer, during changes in tunnel conditions, and at all times when the probes are not in use (Fig. 3).

The probes required for flow-field survey measurements were rake-mounted on the X-Z mechanism (Fig. 3) at the foot of the Z' drive strut that was extended or retracted to accomplish the survey. The angle of the survey strut with respect to the vertical was fixed by manually sweeping the strut to the selected angle between 5 deg (swept upstream) and -15 deg (swept downstream) and locking the strut in position. In the present test, the sweep angle of the strut was set at -8.0 deg for the smaller-gradient model and at -9.0 deg for the larger-gradient model. In either case, the direction of a survey was no more than 2.0 deg from the local normal to the model surface.

A sketch of the survey probe rake is shown in Fig. 4. The top and rear surfaces of the rake were designed to mate to the Z' drive strut of the X-Z Survey Mechanism. The rake was provided with four 0.10-in. I.D. tubes through which were mounted the flow field survey probes. Each tube was fitted with a clamp to hold the probe in position. The outboard tube on either side of the probe rake was located in a removable section (Fig. 4). Several, identical copies of these removable components were available. This feature facilitated the installation and replacement of fragile probes and allowed critical probe alignments to be made in advance under a laboratory microscope, as required for the anemometer probes. Removable sections were also available with a tube diameter of 0.11-in. I.D. to accommodate the hot-film probes.

2.4 FLOW-FIELD SURVEY PROBES

The hot-wire anemometer probes (Fig. 5a) were fabricated by AEDC. Platinum, 10-percent-rhodium wires, drawn by the Wollaston process, of 20-μin. nominal diameter and approximately 140 diameters in length were attached to sharpened 3-mil nickel wire supports using a bonding technique developed by Philco-Ford Corporation (Ref. 12). The wire supports were inserted in an alumina twin-bore cylinder of 0.032-in. O.D. and 0.25-in. length, which was, in turn, cemented to an alumina twin-bore cylinder of 0.063-in. O.D. and 3.0-in. length that carried the hot-wire leads through the probe holder of the survey mechanism. The larger-diameter alumina cylinder was cemented inside a stainless steel sleeve with an O.D. of 0.93 in.

The pitot pressure probe (Fig. 5b) had a cylindrical tip of 0.007-in. inside diameter. This probe was fabricated by cold-drawing a stainless steel tube through a set of wire-drawing dies until the desired inside diam was obtained. The outside surface of the drawn tube was subsequently electropolished to a diameter of 0.015 in. to minimize interference with the flow field surveyed. This tube was telescoped in a succession of larger diameter tubes for installation in the probe rake.

The unshielded total temperature probe was fabricated from a length of sheathed thermocouple wire (0.020-in. O.D.) containing two 0.004-in.-diam wires. The wires were bared for a length of approximately 0.040 in., and a thermocouple junction of approximately 0.008 in. diameter was made. Details of this probe are shown in Fig. 5c.

A hot-film anemometer probe (Fig. 5d) was included among the diagnostic devices used in this test in order to evaluate the capabilities of the film probe for possible applications to future boundary-layer stability studies. The films appear to promise considerably greater durability than the wires described in the earlier paragraph, especially for applications in flows with elevated dynamic pressures (Q greater than 3 psia, say) where air loads cause an unacceptable rate of sensor failures by producing excessive tension in the wires. The hot-film probes were fabricated for AEDC by Dr. A. Demetriades of Montana State University, under a separate project.

The body of the hot-film probe was an alumina twin-bore cylinder of 0.102-in. O.D. and 4.0-in. length. The upstream 15-percent of the body was ground to a wedge shape and capped by a glaze tip which was fused to platinum lead wires inserted in the cylinder. The glaze leading edge was ground and polished to give a wedge tip of approximately 0.02-in. height and 0.07-in. width. The film was applied as a thin line of a liquid platinum resinate solution along the major axis of the probe tip face, from one lead wire to the other. The organic matter of the coating was volatilized by placing the probe in a high-temperature oven, and a film of high-purity platinum remained on the tip.

In addition to the probes used for survey measurements, a "touch-sensor" wire was attached to the probe shield to halt the probe drive mechanism prior to contact of the shield with the model. (See Sections 2.3 and 3.1.) The "touch sensor" was made by brazing a lead wire to a piece of 0.031-in.-O.D. steel tubing. This tubing was telescoped in a larger diameter tube (0.093-in. O.D.) and electrically isolated from the larger tube using Pyroceram® cement. The inner tubing was bent to make contact with the model surface as required.

2.5 TEST INSTRUMENTATION

2.5.1 Standard Instrumentation

The measuring devices, recording devices, and calibration methods for all parameters measured during this test are listed in Table 2. Also, Table 2 identifies the standard wind tunnel instruments and measuring techniques used to define test parameters such as the model attitude, the model surface conditions, probe positions, and probe measurements. Additional special instrumentation used in support of this test effort is discussed in the succeeding subsections.

2.5.2 Model Surface Instrumentation

The locations of the model instrumentation are listed in Table 1. The surface pressure orifices (TAP 1 - TAP 24) on the model had a diameter of 0.040 in., and the pressures were measured using one-psid Druck® transducers or 2.5-psid ESP® transducers included in the Standard Pressure System of Tunnel B.

The Schmidt-Boelter heat-flux gages were fabricated by the AEDC. Each gage consisted of a 0.025-in. diam thick anodized aluminum wafer which was wrapped with 0.002-in.-diam constantan wire. One-half of the wafer was copper-plated, creating a multi-element copper-constantan differential thermocouple. The wire-wound wafer was partially surrounded by an aluminum heat sink, and the top surface of the wafer, adjacent to the air flow over the model, was covered with a thin layer of Epoxy® and then painted with a high-temperature paint. On the inside of each gage, an iron-constantan thermocouple was used to measure the temperature (TG) of the wafer bottom surface. This temperature and the output of the differential thermocouple were used to determine gage surface temperature (TW) and the corresponding heat-transfer rate employing laboratory-calibrated scale factors (See Section 3.3.5.). A more detailed description of the Schmidt-Boelter gage is given in Ref. 13.

2.5.3 Hot-Wire Anemometry Instrumentation

Flow fluctuation measurements were made using hot-wire anemometry techniques. Constant-current hot-wire anemometer instrumentation with auxiliary electronic equipment was furnished by AEDC. The anemometer current control (Philco-Ford Model ADP-13) which supplies the heating current to the sensor is capable of maintaining the current at any one of 15 preset values individually selected using push-button switches. The anemometer amplifier (Philco-Ford Model ADP-12), which amplifies the wire-response signal, contains the circuits required to compensate the signal electronically for thermal lag which is a characteristic of the finite heat capacity of the sensor. A square-wave generator (Shapiro/Edwards Model G-50) was used in determining the time constant of the sensor whenever required. The sensor heating current and mean voltage were fed to autoranging digital voltmeters for a visual display of these two parameters and to a Bell and Howell Model VR3700B magnetic tape machine and to the tunnel data system for recording. The sensor response a-c voltage was fed to an oscilloscope for visual display of the raw signal and to a wave analyzer (Hewlett-Packard Model 8553B/8552B) for visual display of the spectra of the fluctuating signal and was recorded on magnetic tape for subsequent analysis by AEDC. A detailed description of the hot-wire anemometer instrumentation is given in Ref. 14.

The a-c response signal from the hot-wire anemometer probe was recorded using the Bell and Howell Model VR3700B magnetic tape machine in the FM-WBII mode. This channel, when properly calibrated and adjusted, has a signal-to-noise ratio of 35 db at 1 volt rms output and a frequency response of +1 to -3 db over a frequency range of 0 to 500 kHz. A sine wave generator was used to check each channel at several discrete frequencies, using an rms-voltmeter which is periodically calibrated on the 1-, 10-, and 100-volt ranges. The sensor heating current and mean voltage signals from the hot-wire anemometer were also tape-recorded, using the FM-WBI mode. Magnetic tape recordings were made with a tape speed of 60 or 120 in./sec. (See Section 3.2.1.)

2.5.4 Pitot Probe Pressure Instrumentation

Pitot probe pressures were measured during surveys of the model boundary layer using a 15-psid Druck transducer calibrated for 10-psid full scale. As the probe was moved across the boundary layer, the small size of the pitot probe (Section 2.4) required a time delay between points in order to stabilize the pressure within the probe tubing between orifice and transducer. In order to reduce the lag time, the pitot pressure transducer was housed in a water-cooled package attached to the trailing edge of the strut on which the probe rake was mounted (Section 2.3). The distance between orifice and transducer was approximately 18 in. The resultant lag time was about one second.

2.5.5 Hot-Film Anemometry Instrumentation

For flow fluctuation measurements made with hot-film probes, constant-current anemometry techniques were used. Higher currents are generally required to heat the film sensor to sensitivies comparable to those used with the hot wire. A special current control circuit was prepared by AEDC which differed from the Philco-Ford Model ADP-13, used with the hot-wire probes, in being able to supply higher values of current to heat the sensor. The anemometer amplifier used with the hot-film measurements was a Philco-Ford Model ADP-12, identical in design to the amplifier used with the hot-wire probe. The auxiliary instrumentation used to measure and record the hot-film signals was the same as that used with the hot-wire probes, as described in Section 2.5.3.

A simple method for determining the time constant of the film sensor with its substrate is not yet available. In the present effort, the value of time constant which was set in the compensation stage of the amplifier was estimated rather than measured. However, the settings should allow qualitative evaluation of the film performance at the high frequencies characteristic of the laminar disturbances in hypersonic boundary layers. This evaluation is beyond the scope of the present report.

3.0 TEST DESCRIPTION

3.1 TEST CONDITIONS AND PROCEDURES

A summary of the nominal test conditions is given below.

M	PT, psia	TT, °R	V, ft/sec	Q, psia	T, °R	P, psia	RE/FT x 10^{-6}
7.94	225	1310	3855	1.06	98	0.024	1.0
7.96	340	1310	3857	1.58	98	0.036	1.5
7.98	453	1310	3859	2.10	97	0.047	2.0

A summary of the test runs for the present measurements using the two pressure gradient models is given in Table 3. Boundary-layer measurements were made only at RE/FT = 1.0 million.

In the continuous-flow Tunnel B, the model is mounted on a sting support mechanism in an installation tank directly underneath the tunnel test section. The tank is separated from the tunnel by a pair of fairing doors and a safety door. When closed, the fairing doors, except for a slot for the pitch sector, cover the opening to the tank, and the safety door seals the tunnel from the tank area. After the model is prepared for a data run, the personnel access door to the installation tank is closed, the tank is vented to the tunnel flow, the safety and fairing doors are opened, the model is injected into the airstream, and the fairing doors are closed. After the data are obtained, the sequence is reversed; the model is retracted into the tank which is then vented to atmosphere to allow access to the model in preparation for the next run. The sequence is repeated for each configuration change.

Probes mounted to the X-Z mechanism (Section 2.3) are deployed for measurements by the following sequence of operations: the air lock is closed, secured over the mechanism, and evacuated; and the access door to the tunnel test section is opened. The various drive systems are used to inject the probes into the test section and position the probes at a designated survey station along the length of the model, the shield protecting the probes is raised exposing them to the flow, and the flow field is traversed to selected probe heights. When the traverse has been concluded, the shield is closed over the probes, and the mechanism is repositioned along the model. When the surveys are completed or when a probe is to be replaced, the X-Z Mechanism is retracted from the flow, and the test section access door is closed. The air lock is then vented to atmosphere and opened to allow personnel access to the mechanism.

The survey probe height relative to the model was monitored using a high-magnification, closed-circuit television (CCTV) system. The video camera was fitted with a telescopic lens system which gave a magnification factor of 20 for the monitor image. The probe and model were back-lighted using the collimated light beam from the Tunnel B shadowgraph system which produced high-contrast silhouettes of the model and probe (Fig. 6). The camera was mounted on a horizontal-vertical traversing mount to facilitate alignment of the camera with the probe at various model stations visible through the test section windows. The video camera was interfaced with an image analyzer/digitizer system which was used to measure the distance between the probe and model surface using computer-assisted image analysis techniques. For each measurement the lower edge of the probe and the upper edge of the model surface were located by an operator using a cursor with the video image. The system was calibrated prior to testing by the same operator using the same technique to locate edges separated by a known distance.

A hardcopy of the video image of the probes and model edge was provided in near real-time, showing, by means of a graphics line, the location of the edges measured and displaying a printout of the measured distance and other pertinent information. The accuracy of this measurement technique was determined to be better than ±0.0007-in. over a range of 0.003 to 0.2 in. under air-off conditions. The video images used for test measurements were recorded on disk for post test review, if needed.

The flow-field surveys were accomplished in the following sequence: (1) the survey mechanism was positioned at the desired model axial station (XSTA) by the controller operating in either manual or automatic mode and locked in axial position, (2) the survey mechanism was driven downward toward the surface by the controller until the "touch-sensor" wire (Section 2.4) attached to the probe shield made contact with the model surface, (3) final adjustments of probe instrumentation were made and the shield was raised, (4) the survey mechanism was driven toward the model surface by the controller in the manual mode to a position close to (generally 0.040 to 0.060 in. above) the surface, (5) measurements of probe positions relative to the surface and to each other were made using the image analyzer and the information was manually entered into the data system, (6) the probes were traversed across the flow field in selected increments by the controller in the manual mode to acquire the desired data, (7) the axial position of the survey mechanism was unlocked and the mechanism was repositioned at the next survey station along the model.

3.2 DATA ACQUISITION

The primary test technique used in the present investigation of the development of instabilities in a laminar boundary layer was hot-wire anemometry. In addition, mean-flow boundary-layer profile data (pitot pressure and total temperature profiles) were acquired in order to define the flow environment in the vicinity of the hot-wire. All boundary-layer measurements were made above the top (zero) ray of the model. Surface pressures and temperatures on the model were measured to supplement the profile data. The various types of data acquired are summarized in Table 3. Model stations for surveys are listed in Tables 3a and 3b.

3.2.1 Anemometry Data

The hot-wire anemometer data acquired during the present testing were of two general categories: (1) continuous-traverse surveys of the boundary layer to map the response of the hot-wire anemometer as a function of distance from the surface and (2) discrete-point hot-wire measurements using the wire operated at one or eleven wire heating currents at one or more locations on a profile.

Data of the first category were acquired with the hot wire operated using a single heating current, in the present case the maximum (practical) current. The probe was generally translated in a continuous manner from near the model surface outward beyond the edge of the boundary layer. These data were recorded only as analog plots of the hot-wire response (rms of the a-c voltage component) versus probe height above the model surface. The plot was used primarily for the purpose of determining the station in the boundary-layer profile where the hot-wire output reached a maximum value.

Discrete-point hot-wire data (second category) were acquired at locations determined from the continuous-traverse surveys (first category data). The point of maximum rms voltage output of the hot wire, the "maximum energy point" of the profile, was selected for quantitative measurements at each model station. The quantitative data were acquired using each of eleven wire heating currents; one current was nominal-zero to obtain a measurement of the electronic noise of the anemometer instrumentation. Each wire heating current, wire mean voltage (d-c component) and the rms value of the wire voltage fluctuation (a-c component) were measured 40 times using the Tunnel B data system. At the same time, the hot-wire parameters were recorded (generally, a five-second record duration) on magnetic tape with a tape transport speed of 120 in./sec.

Discrete-point hot-wire data were also obtained simultaneously with certain of the boundary-layer mean-flow profile data (Section 3.2.2). In this case a measurement and recording of the electronic noise was made only at the start of the traverse and was assumed to be valid for all points of the profile. At the other points of the traverse the hot wire was operated at the maximum heating current selected for the first category data. The tape recording duration was 5 sec at each point and a tape transport speed of 60 in./sec was used.

Hot-film probe data were acquired simultaneously with the hot-wire measurements. However, the hot-wire and hot-film sensors generally were not at the same height above the surface of the model during acquisition of a set of measurements. Therefore, the sensors were exposed to different values of flow disturbance. Specifically, when the hot wire was at the location of maximum disturbance energy, the hot film was located at a point of less disturbance energy. As a result, comparison of the response signals of the two sensors generally must be confined to their spectra. Such comparisons are beyond the scope of this report.

3.2.2 Profile and Surface Data

Mean-flow boundary-layer profiles generally extended from a height of 0.04 to 0.06 in. above the model surface to a distance of 1.5 times the boundary-layer total thickness. A profile typically consisted of 40 data points (heights). The probe direction of travel was at an angle of 8.0 or 9.0 deg with respect to the vertical, depending on the model configuration. (See Section 2.3).

Model surface pressures, temperature distributions, and heat-flux distributions were acquired to supplement the boundary-layer surveys. The surface pressures and temperatures were monitored throughout the test.

3.2.3 Anemometer and Total Temperature Probe Calibrations

The evaluation of flow fluctuation quantitative measurements made using hot-wire anemometry techniques requires a knowledge of certain thermal and physical characteristics of the wire sensor employed. In the application of the hot wire to wind tunnel tests, two complementary calibrations are used to evaluate the wire characteristics needed. The first calibration of each hot-wire probe is performed in the instrumentation laboratory prior to the testing: the probe is placed in an oven, and the resistance of the wire at zero heating current is determined at up to 27 oven temperatures between room temperature and 600°F. The wire reference resistance at 32°F and the thermal coefficient of resistance, also at 32°F, are obtained from the results; the wire aspect (length-to-diameter) ratio is determined, using the wire resistance per unit length specified by the manufacturer with each supply of wire. Moreover, it has been established that the exposure of the probes to the elevated temperatures of the oven calibration often serves to eliminate probes with inherent weaknesses.

Hot-wire probes used for flow-field measurements are also calibrated in the wind tunnel free-stream flow to obtain both the heat-loss coefficient (Nusselt number) and the temperature recovery factor characteristics of the wire sensor as functions of Reynolds number. The variations of Reynolds number in the free stream are obtained by varying the tunnel total pressure (PT) while holding the tunnel total temperature (TT) at a nominally constant valve. The resulting relationships are used to determine the values of the various wire sensitivity parameters required in the reduction of the quantitative measurements.

Identical calibration procedures are used with hot-film probes in the oven and in the tunnel free-stream flow to evaluate film thermal characteristics. For the present test, three hot-wire probes and three hot-film probes were calibrated in the Tunnel B test section flow. (See Table 3c.) Several additional probes of both types were oven-calibrated in anticipation of their use in the testing.

A calibration of the recovery factor of two total-temperature probes as a function of Reynolds number was made in the free-stream flow of the tunnel test section simultaneously with the calibration of the anemometer probes. The local total temperature for the probes in free-stream flow was assumed to be equal to the measured stilling chamber temperature, TT (see Section 3.3.4).

3.3 DATA REDUCTION

3.3.1 Anemometry Data

In the present discussion of the reduction of anemometer data, only the basic measurements tabulated in the data package that accompanies this report will be considered. (Examples of the tabulations are shown in the Sample Data.) The data processing associated with spectral analysis, modal analysis, and determination of amplification rates of laminar disturbances is beyond the scope of this report. However, extended data reduction of the present hot-wire results to achieve these analyses is planned.

The basic measurements associated with quantitative hot-wire data are the following parameters: wire heating current (CURRENT), wire mean voltage (EBAR), and the rms value of the wire fluctuating response voltage (ERMSA). The average value of 40 measurements of each of the three parameters was determined for each of the 11 nominal wire heating currents employed, and the results were tabulated under the designation "DATA TYPE 9" together with certain associated model, flow field, and tunnel conditions. (See Sample 1.) Similarly, the basic parameters of the hot-film data are the film heating current, the film mean voltage, and the rms value of the film a-c response voltage (ERMSF). Each of these parameters was measured 40 times for each of the 11 nominal film heating currents and the average values were tabulated on the second page of the DATA TYPE 9 results.

Free-stream tunnel conditions that are applicable to anemometer and total-temperature probe calibrations are tabulated under the designation "DATA TYPE 6." (See Sample 2.)

3.3.2 Flow-Field Survey Data

The mean flow-field data reduction included calculation of the local Mach number and other local flow parameters, determination of the height of each probe relative to the model surface, correction of the total-temperature probe measurements using the recovery factor calibration (Section 3.2.3), definition of the boundary-layer total thickness, and evaluation of the displacement and momentum thicknesses. Sample tabulated data are shown in Sample 3, and typical plotted results are shown in Fig. 7. The data reduction procedures are outlined as follows.

The local Mach number in the flow field adjacent to the model was determined using the measured pitot pressure (PP) and the model static pressure (PWL). The pressure distribution on each model configuration is shown in Fig. 8.

The height of each probe above the model surface was calculated for each point in a given flow-field survey, taking into consideration the following parameters: the initial distance determined from the CCTV image, the distance traversed from the initial position employing the survey probe drive, the lateral displacement of the probe from the vertical plane of symmetry of the model, and the local radius of the model at the station of the flow-field survey.

The height of the pitot pressure probe above the model surface (ZP) was used as the reference for all probes. The recovery temperature measurements (TTTU) of the total temperature probe were used to interpolate a value (TTLU) corresponding to each height of the pitot probe. Correction of the interpolated recovery temperature, using the probe calibration data, was achieved by iteration on the local Reynolds number (LRET) beginning with the value calculated using the recovery temperature (TTLU) to determine an initial value for the local dynamic viscosity (MUTTL). The iteration was continued until successive values of the "corrected" total temperature differed by no more than 0.1°R. For those surveys wherein the pitot probe was positioned below the total-temperature probe (closer to the model surface), the corrected total temperature at the corresponding pitot probe heights was determined from a second-order curve fit using three points, namely: the model surface temperature (TWL) and the corrected total temperature at the first two probe heights.

The total thickness of the model boundary layer in any given profile was inferred from the profile of the total-temperature probe corrected temperature (TTL). Total temperatures measured above the edge of the boundary layer (in the shock layer) remained constant or essentially independent of the probe height. There was generally a distinct "overshoot" in the total temperature profile immediately before the onset of the constant portion of the profile. The height at which this constant portion of the profile began, the distance to the model surface, was defined as the boundary-layer total thickness (DEL). Displacement and momentum thicknesses were determined by integration accounting for the local radius of curvature of the model.

3.3.3 Model Surface Pressure and Temperature Data

Model surface pressures and temperatures were tabulated under the designation "DATA TYPE 2" and "DATA TYPE 4." The data presented as DATA TYPE 2 (see Sample 4) represent a single measurement of each pressure and each temperature. These data were, in general, acquired when the survey probes were positioned to minimize interference with the surface measurements.

Model surface measurements were also included among the DATA TYPE 4 results. In this case, surface conditions were measured each time that probe data were acquired. The surface data presented in these tabulations represent the average of the values measured at each orifice and each thermocouple. It should be noted that pressures along the 0-, 90-, and 270-deg rays at X = 38 in. were often influenced by the presence of the survey probes and the Z' survey strut. The extent of the influence was governed by the location of the probes above the model. It is recommended in general that only the pressures measured along the 180-deg ray be used from the surface data tabulated under DATA TYPE 4.

The model surface pressure, PWL, used in the boundary-layer calculations was determined using a fairing of the pressures measured during the test. (See Fig. 8.) The static pressure was assumed to be constant across the boundary layer along the track of any given survey.

3.3.4 Total Temperature Probe Calibration Data

The recovery factor ETA used in reducing the total temperature probe survey data was defined as a function of the local Reynolds number based on the nominal diameter of the thermocouple junction. Free-stream tunnel conditions that are applicable to the total-temperature probe calibration are tabulated under the designation "DATA TYPE 6" (Sample 2.)

3.3.5 Heat-Transfer Data

Data measurements obtained from Schmidt-Boelter gages consisted of the gage voltage (E) and the embedded thermocouple temperature (TG). The gage output is converted to heating rate by means of a laboratory-calibrated scale factor (CSF)

$$QDOT = (CSF)(E) \tag{2}$$

The gage wall temperature was obtained from both the embedded thermocouple temperature (TG) and the temperature difference (ΔT) across the wafer (See Ref. 13). The temperature difference (ΔT) is proportional to the gage output voltage (E)

$$\Delta T = (K)(E) \tag{3}$$

The gage wall temperature is

$$TW = TG + \Delta T \tag{4}$$

The heat transfer coefficient, H(TT), based on tunnel stilling chamber temperature was then computed as

$$H(TT) = \frac{QDOT}{(TT - TW)} \tag{5}$$

An example of the tabulated heat transfer data is shown in Sample 5.

3.4 MEASUREMENT UNCERTAINTIES

In general, instrumentation calibrations and data uncertainty estimates were made using methods presented in Ref. 15. Measurement uncertainty (U) is a combination of bias and precision errors defined as

$$U = \pm\left(B + t_{95} S\right) \tag{6}$$

where B is the bias limit, S is the standard deviation, and t_{95} is the 95th percentile point for the two-tailed Student's "t" distribution, which equals approximately 2 for degrees of freedom greater than 30.

Estimates of the measured data uncertainties for this test are given in Table 2. In general, measurement uncertainties are determined from in-place calibrations through the data recording system and data reduction program. The propagation of the estimated bias and precision errors of the measured data through the data reduction was determined for free-stream parameters in accordance with Ref. 15, and is summarized in Table 4.

4.0 DATA PACKAGE PRESENTATION

Basic hot-wire and hot-film anemometer data, boundary-layer profile data, and model surface data from the test were reduced to tabular and graphical form for presentation as a Data Package. Examples of the basic data tabulations are shown in the Sample Data.

REFERENCES

1. Siler, L. G. and Donaldson, J. C. "Boundary-Layer Measurements on Slender Blunt Cones at Free-Stream Mach Number 8." AEDC-TSR-79-V71 (AD-A085712), December 1979.

2. Donaldson, J. C. and Simons, S. A. "Investigation of the Development of Laminar Boundary-Layer Instabilities Along a Sharp Cone." AEDC-TSR-85-V16 (AD-A159370), April 1985.

3. Donaldson, J. C. and Simons, S. A. "Investigation of the Development of Laminar Boundary-layer Instabilities Along a Blunted Cone." AEDC-TSR-86-V46 (AD-A202425), December 1988.

4. Donaldson, J. C. and Hatcher, M. G. "Investigation of the Development of Laminar Boundary-Layer Instabilities Along a Cooled-Wall Cone in Hypersonic Flows." AEDC-TSR-88-V32 (AD-A202587), December 1988.

5. Donaldson, J. C. and Sinclair, D. W. Investigation of the Development of Laminar Boundary-Layer Instabilities Along a Cooled-Wall Hollow Cylinder at Mach Number 8." AEDC-TSR-89-V25 (AD-A217672), January 1990.

6. Stetson, K. F., Thompson, E. R., Donaldson, J. C., and Siler, L. G. "Laminar Boundary-Layer Stability Experiments on a Cone at Mach 8, Part 1: Sharp Cone." AIAA Paper No. 83-1761, July 1983.

7. Stetson, K. F., Thompson, E. R., Donaldson J. C., and Siler, L. G. "Laminar Boundary-Layer Stability Experiments on a Cone at Mach 8, Part 2: Blunt Cone." AIAA Paper No. 84-0006, January 1984.

8. Stetson, K. F., Thompson, E. R., Donaldson J. C., and Siler, L. G. "Laminar Boundary-Layer Stability Experiments on a Cone at Mach 8, Part 3: Sharp Cone at Angle of Attack." AIAA Paper No. 85-0492, January 1985.

9. Stetson, K. F., Thompson, E. R., Donaldson J. C., and Siler, L. G. "Laminar Boundary-Layer Stability Experiments on a Cone at Mach 8, Part 4: On Unit Reynolds Number and Environmental Effects." AIAA Paper No. 86-1087, May 1986.

10. Stetson, K. F., Thompson, E. R., Donaldson, J. C., and Siler, L. G. "Laminar Boundary-Layer Stability Experiments on a Cone at Mach 8, Part 5: Tests with a Cooled Model." AIAA Paper No. 89-1895, June 1989.

11. Boudreau, A. H. "Performance and Operational Characteristics of AEDC/VKF Tunnels A, B, and C." AEDC-TR-80-48 (AD-A102614), July 1981.

12. Doughman, E. L. "Development of a Hot-Wire Anemometer for Hypersonic Turbulent Flows." Philco-Ford Corporation Publication No. U-4944, December 1971; and The Review of Scientific Instruments, Vol. 43, No. 8, August 1972, pp. 1200-1202.

13. Kidd, C. T. "A Durable, Intermediate Temperature, Direct Reading Heat-Flux Transducer for Measurements in Continuous Wind Tunnels." AEDC-TR-81-19 (AD-A107729), November 1981.

14. Donaldson, J. C., Nelson, C. G., and O'Hare, J. E. "The Development of Hot-Wire Anemometer Test Capabilities for $M_\infty = 6$ and $M_\infty = 8$ Applications." AEDC-TR-76-88 (AD-A029570), September 1976.

15. Abernethy, R. B. et al., and Thompson, J. W. "Handbook Uncertainty in Gas Turbine Measurements." AEDC-TR-73-5 (AD755356), February 1973.

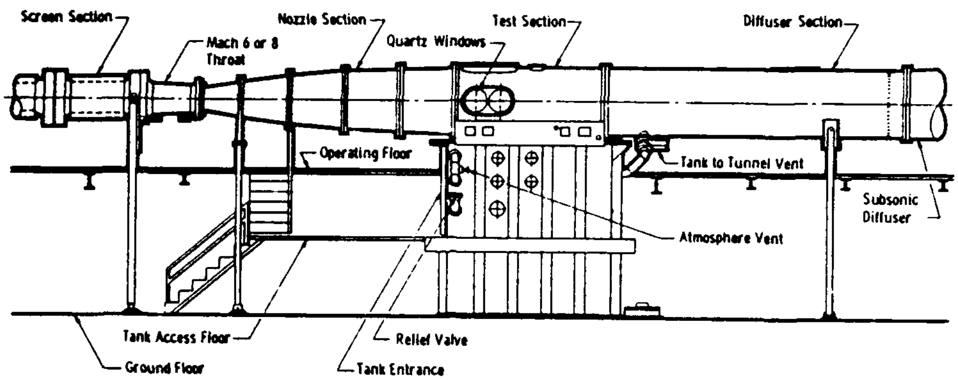

a. Tunnel assembly

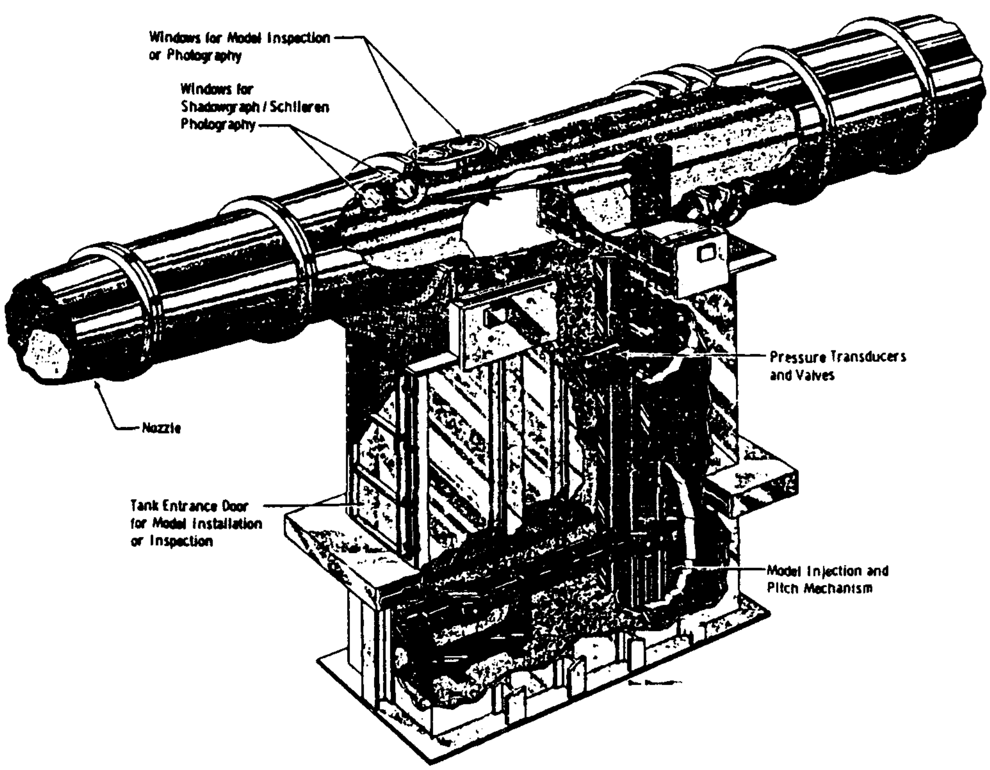

b. Tunnel test section

Figure 1. AEDC Hypersonic Wind Tunnel B

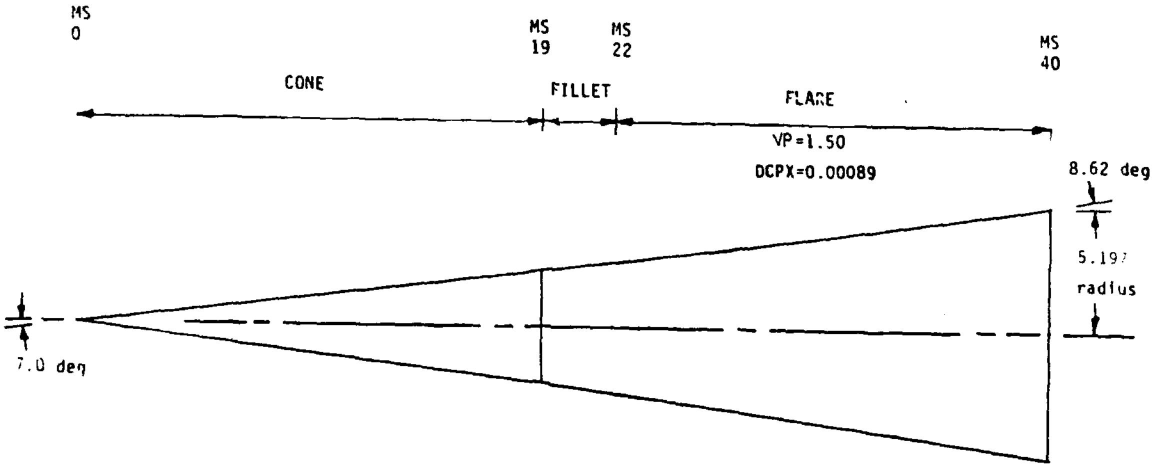

a. Configuration DP/DX : 1

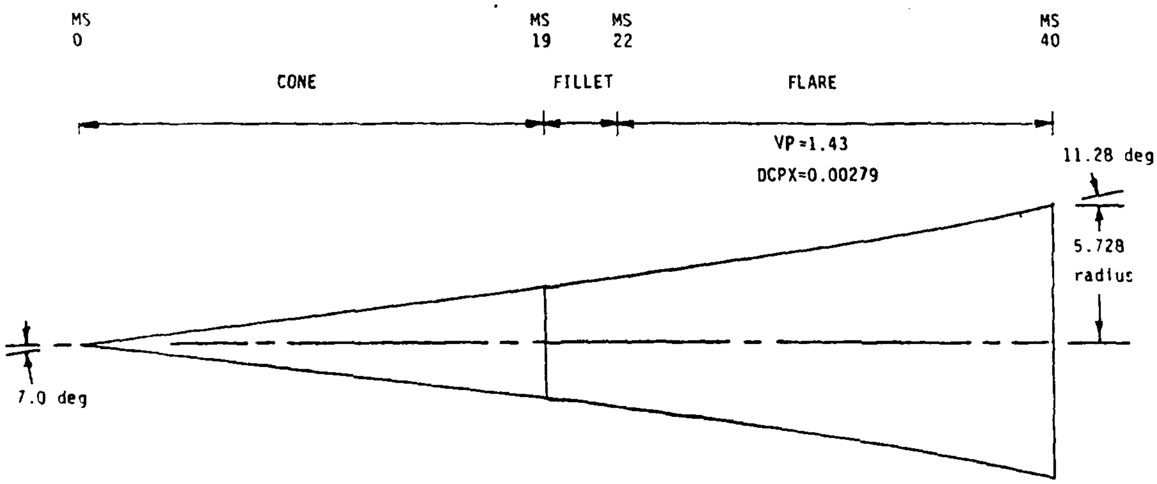

b. Configuration DP/DX : 4

Figure 2. Model Geometry

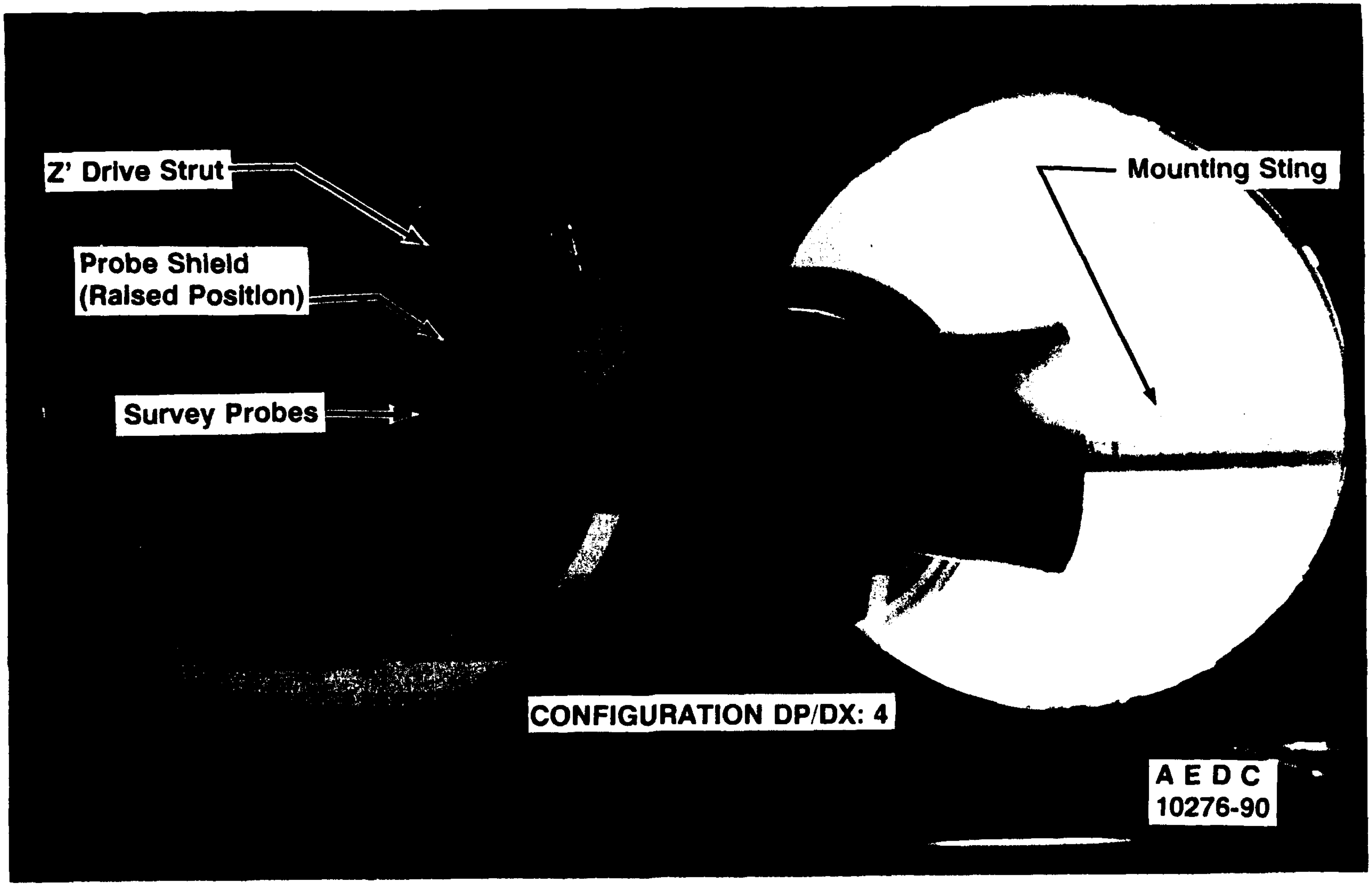

Figure 3. Test Installation

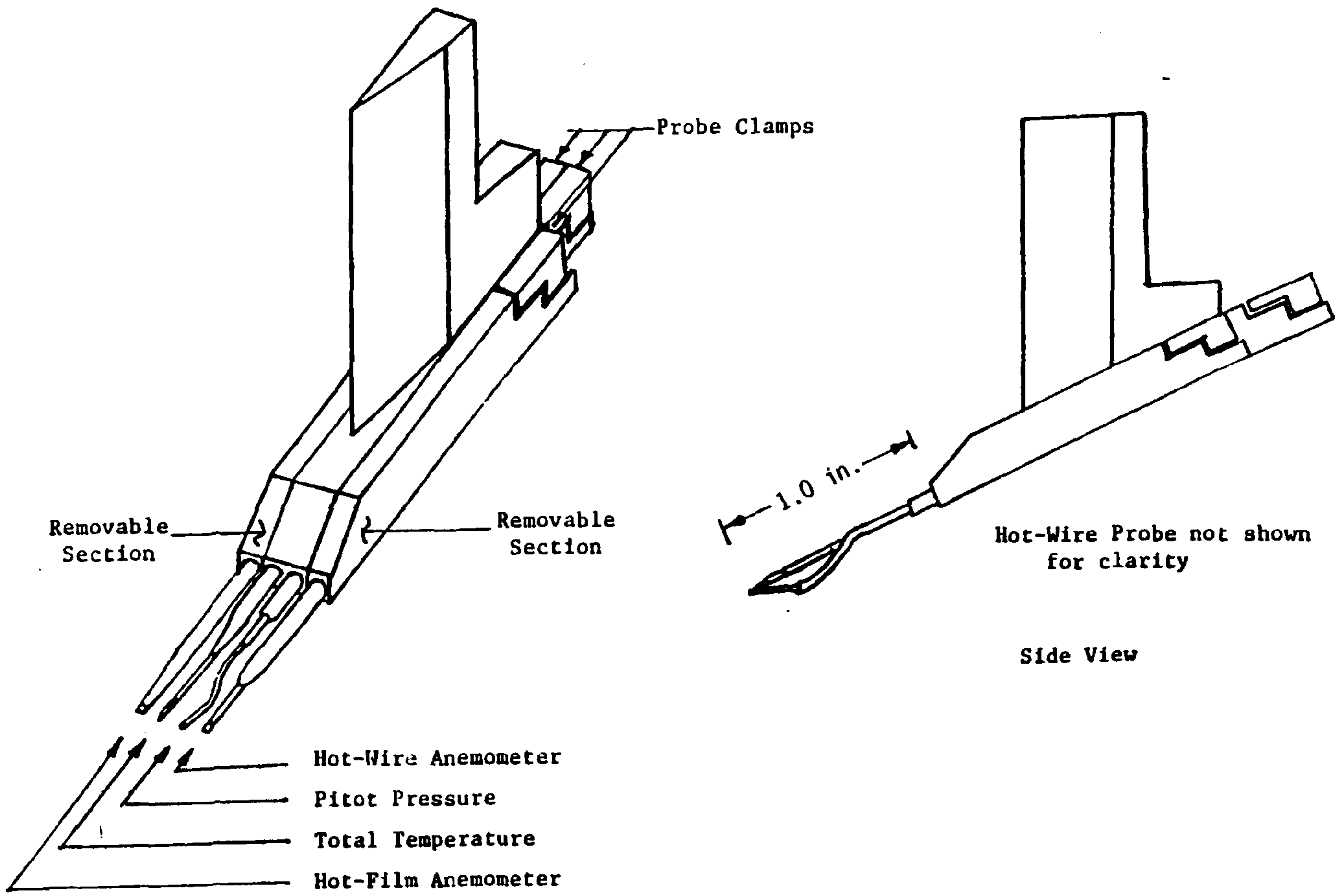

a. Survey Rake Details

Figure 4. Survey Probe Rake

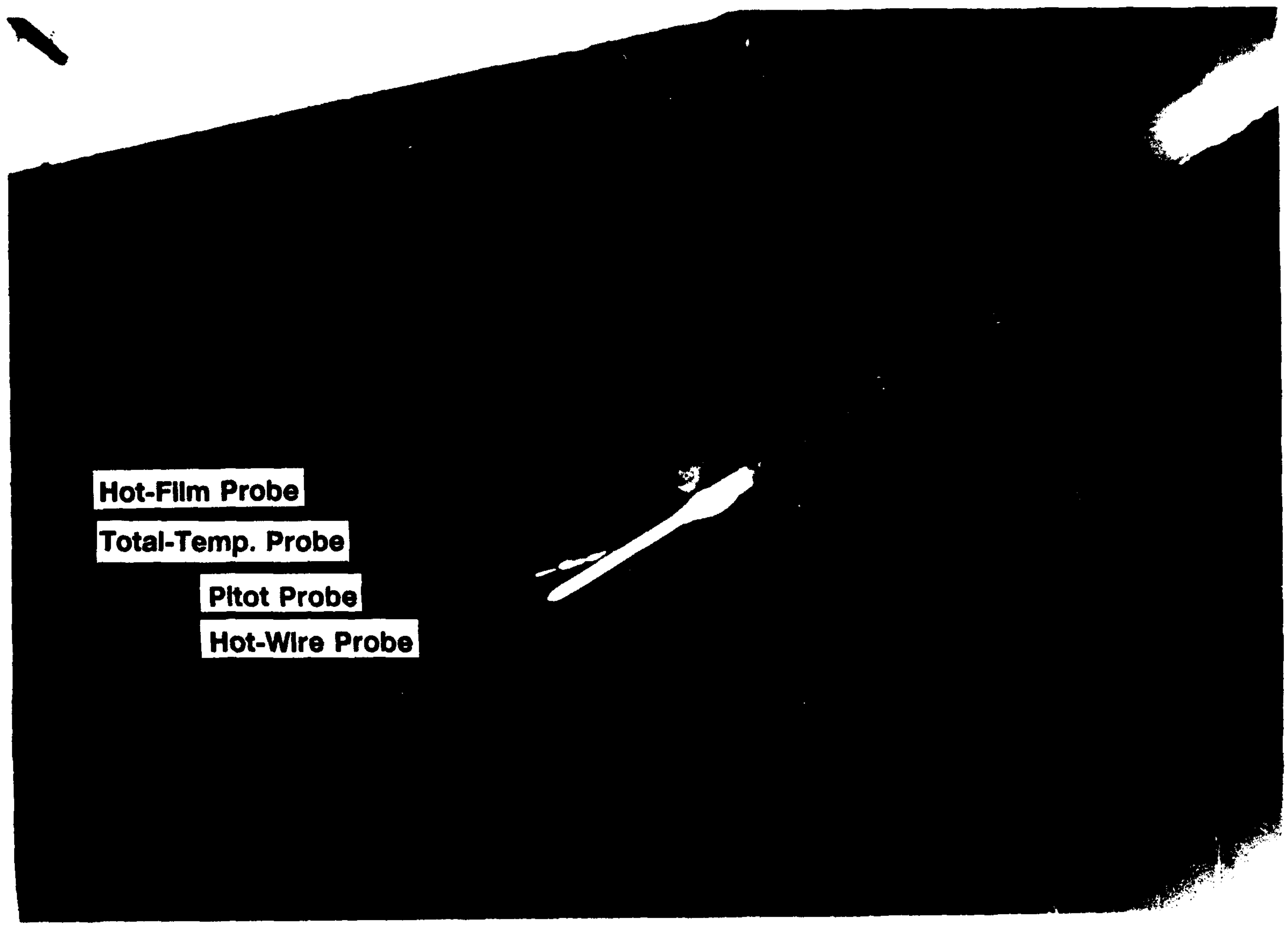

b. Assembled Probes

Figure 4. Concluded

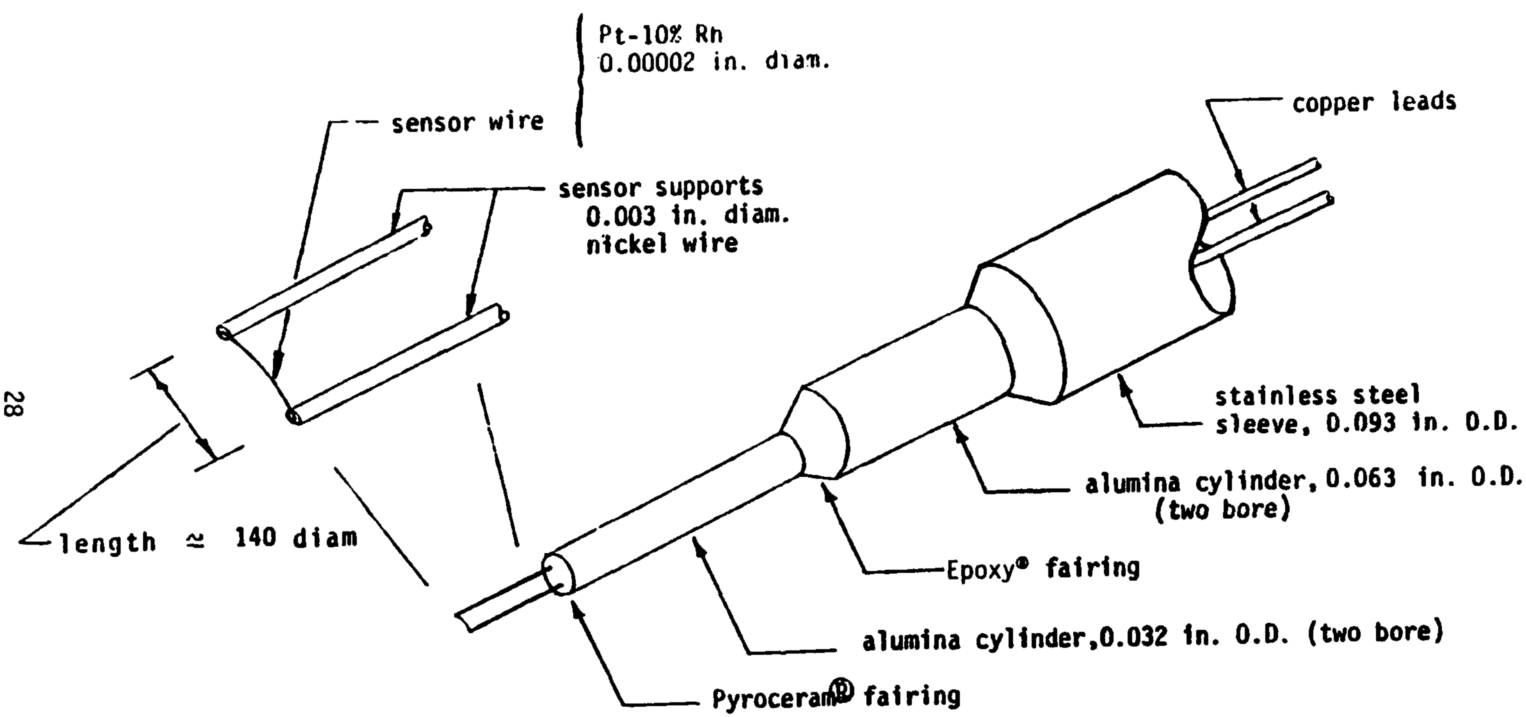

a. Hot-Wire Anemometer Probe

Figure 5. Probe Details

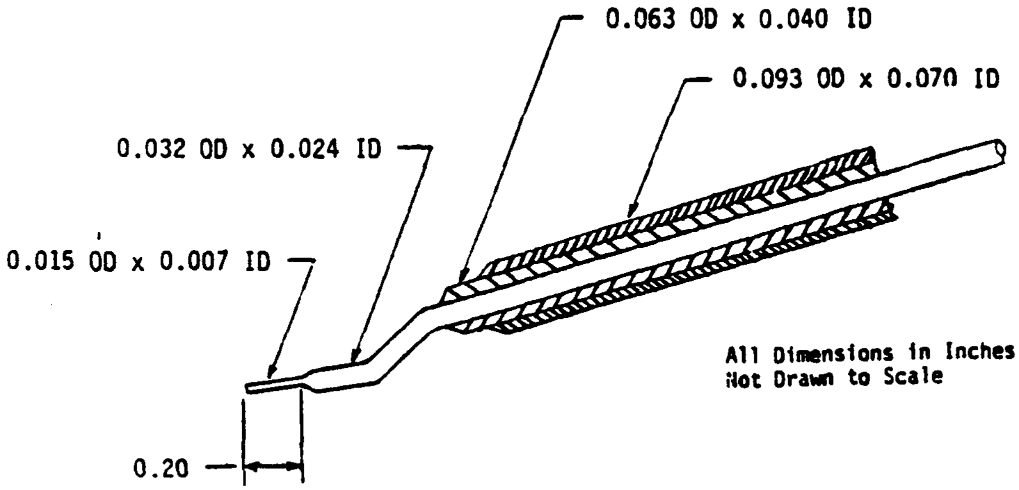

b. Pitot Pressure Probe

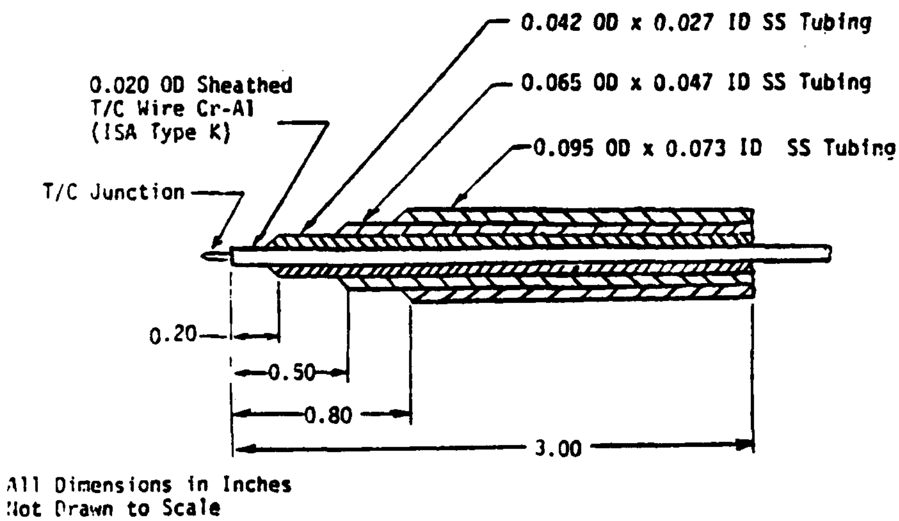

c. Total Temperature Probe

Figure 5. Continued

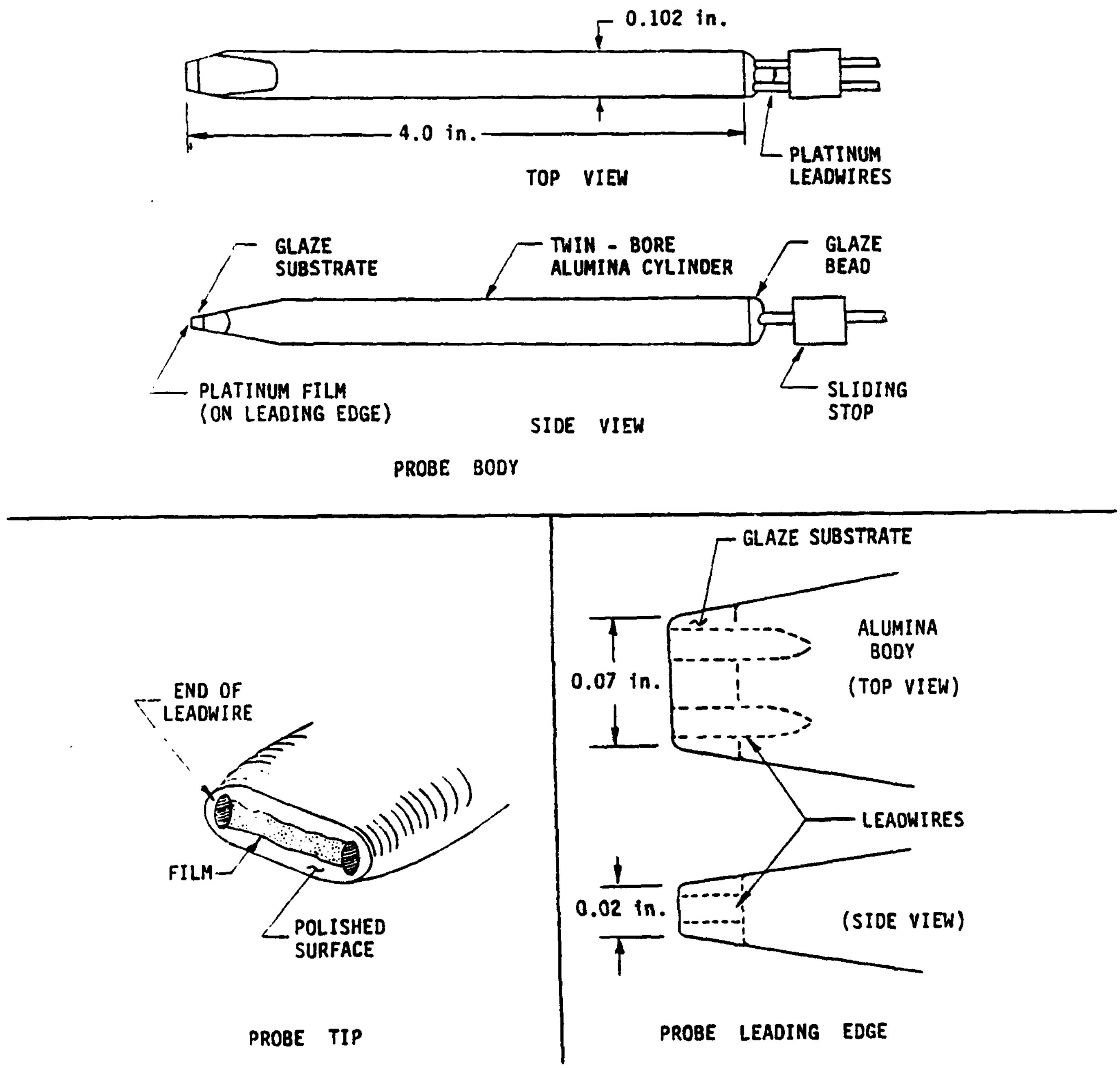

d. Hot-Film Anemometer Probe

Figure 5. Concluded

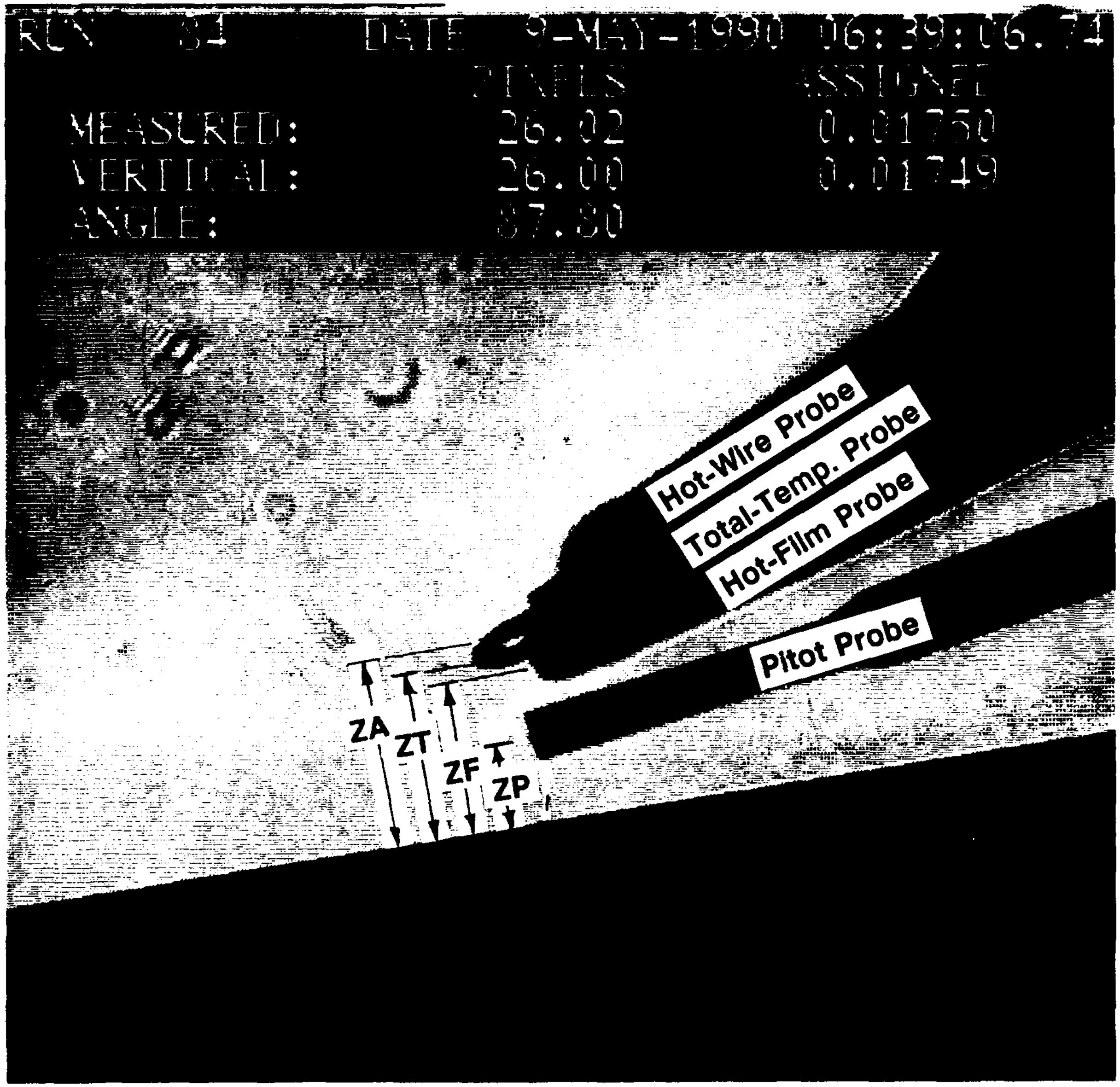

Figure 6. Video Image of Probe and Model Edges

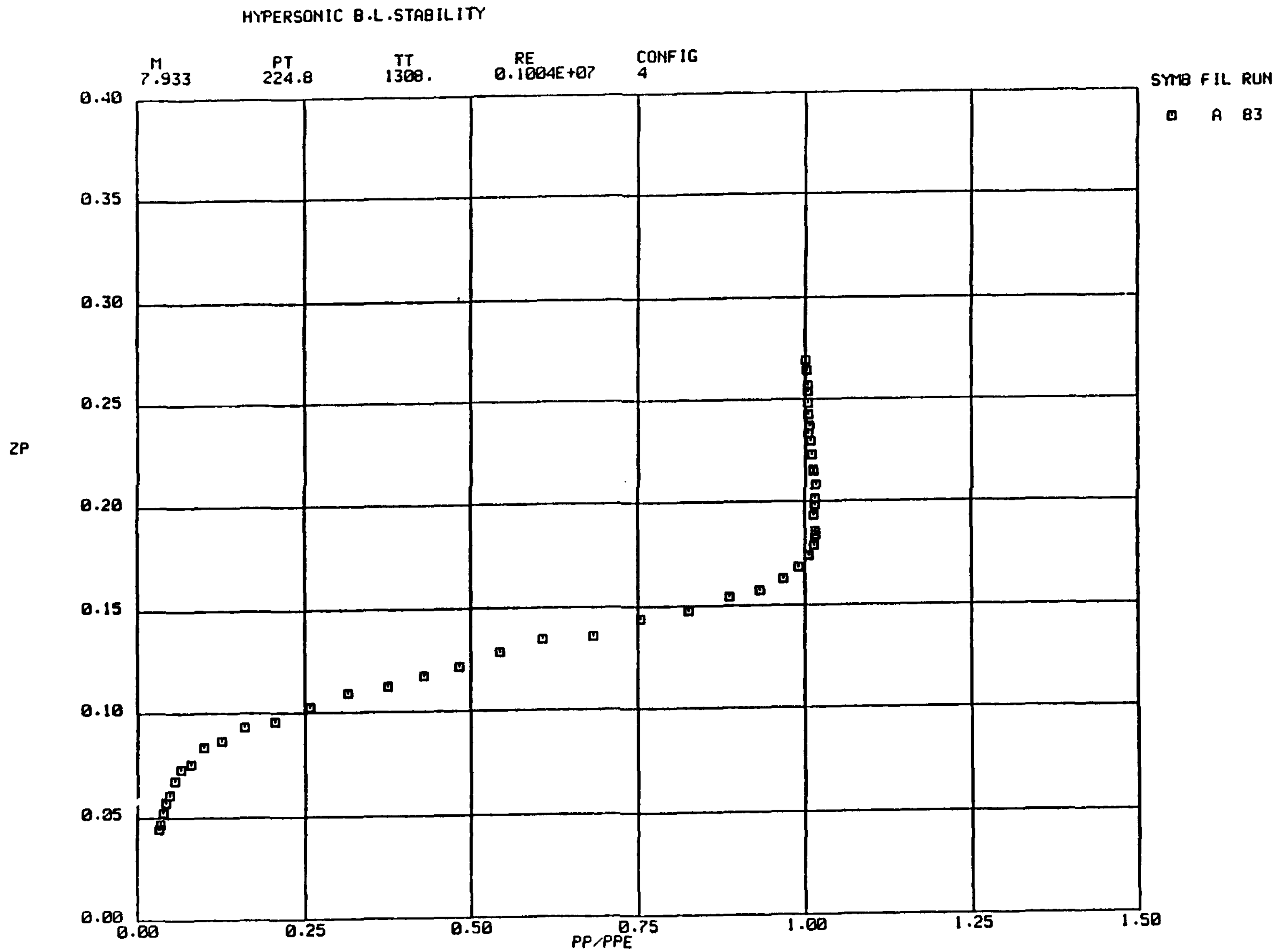

Figure 7. Typical Results of a Boundary-Layer Survey

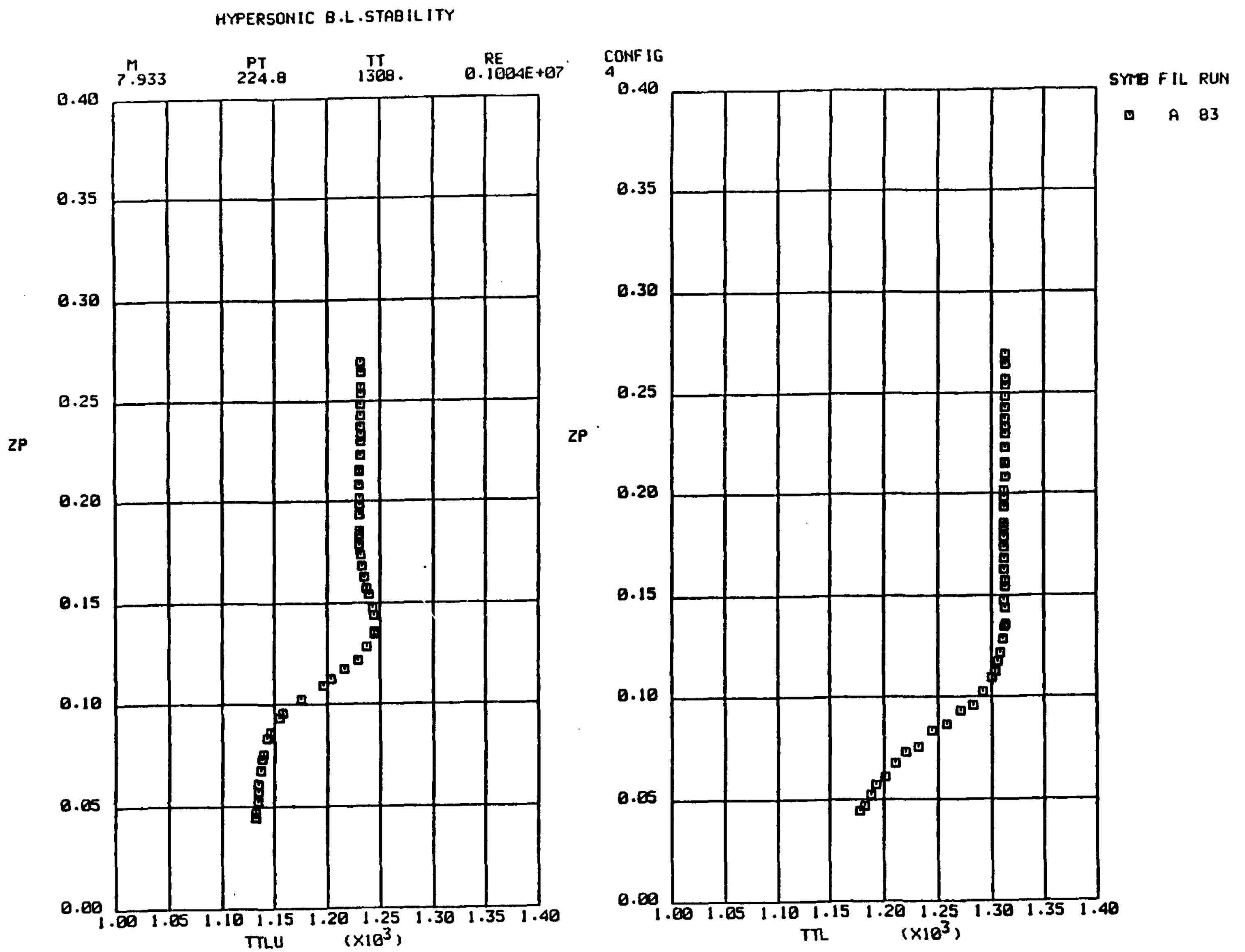

Figure 7. Continued

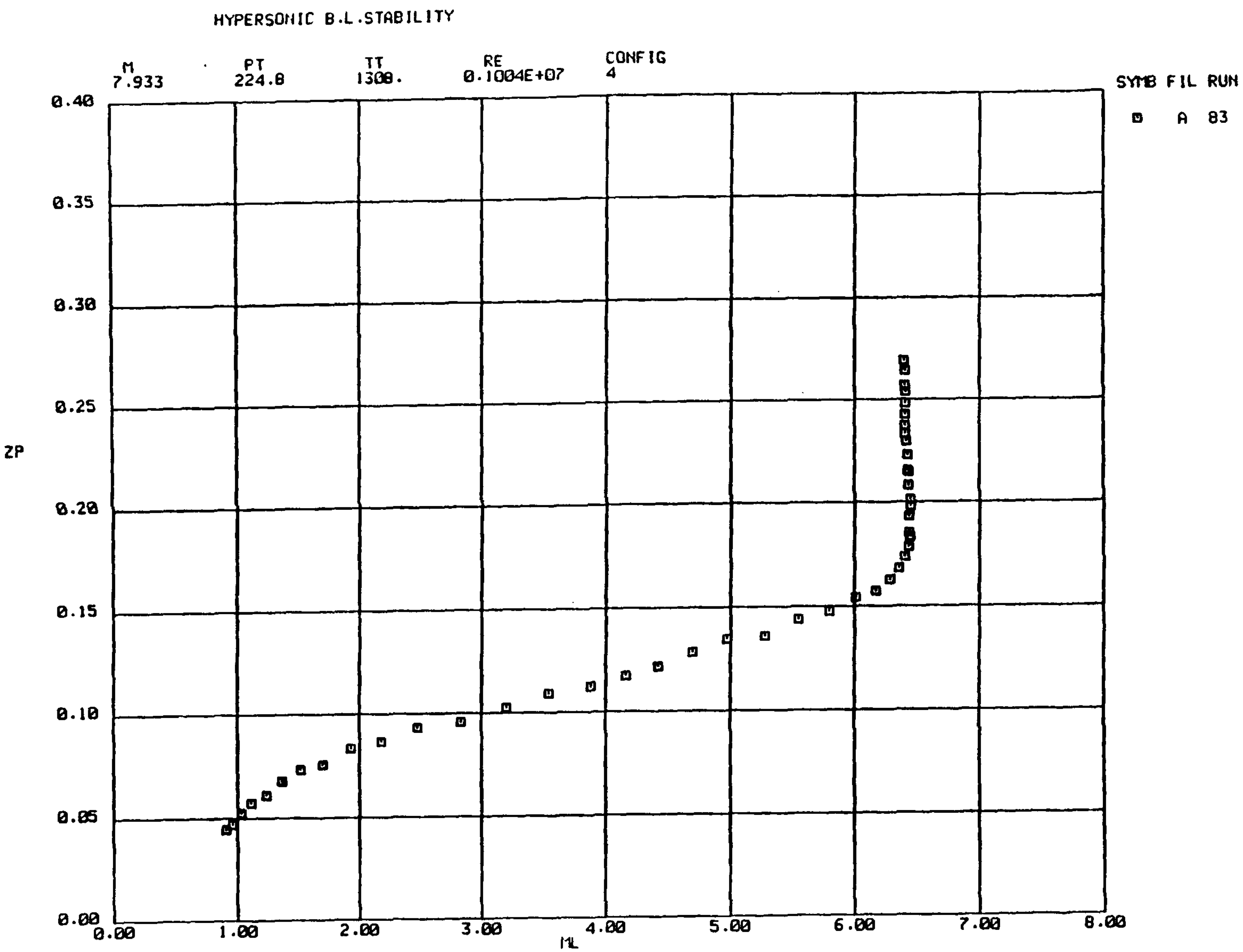

Figure 7. Concluded

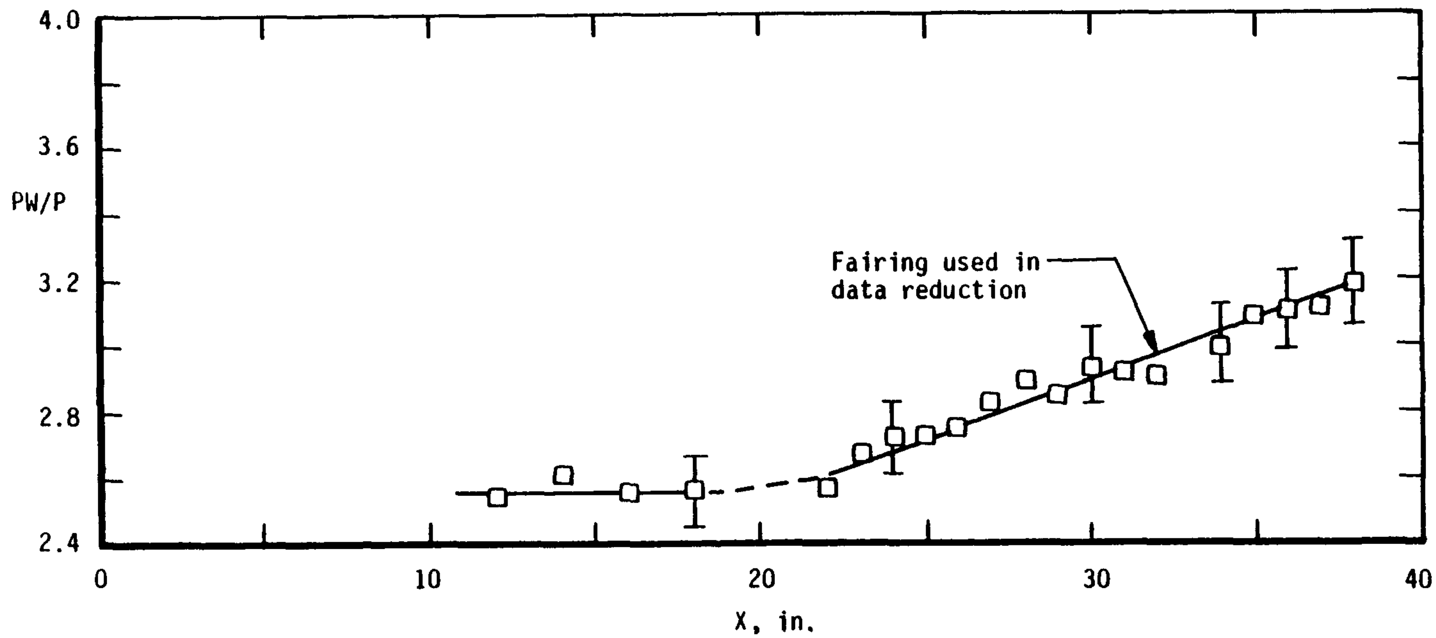

a. Configuration DP/DX : 1

Figure 8. Model Surface Pressure Distributions

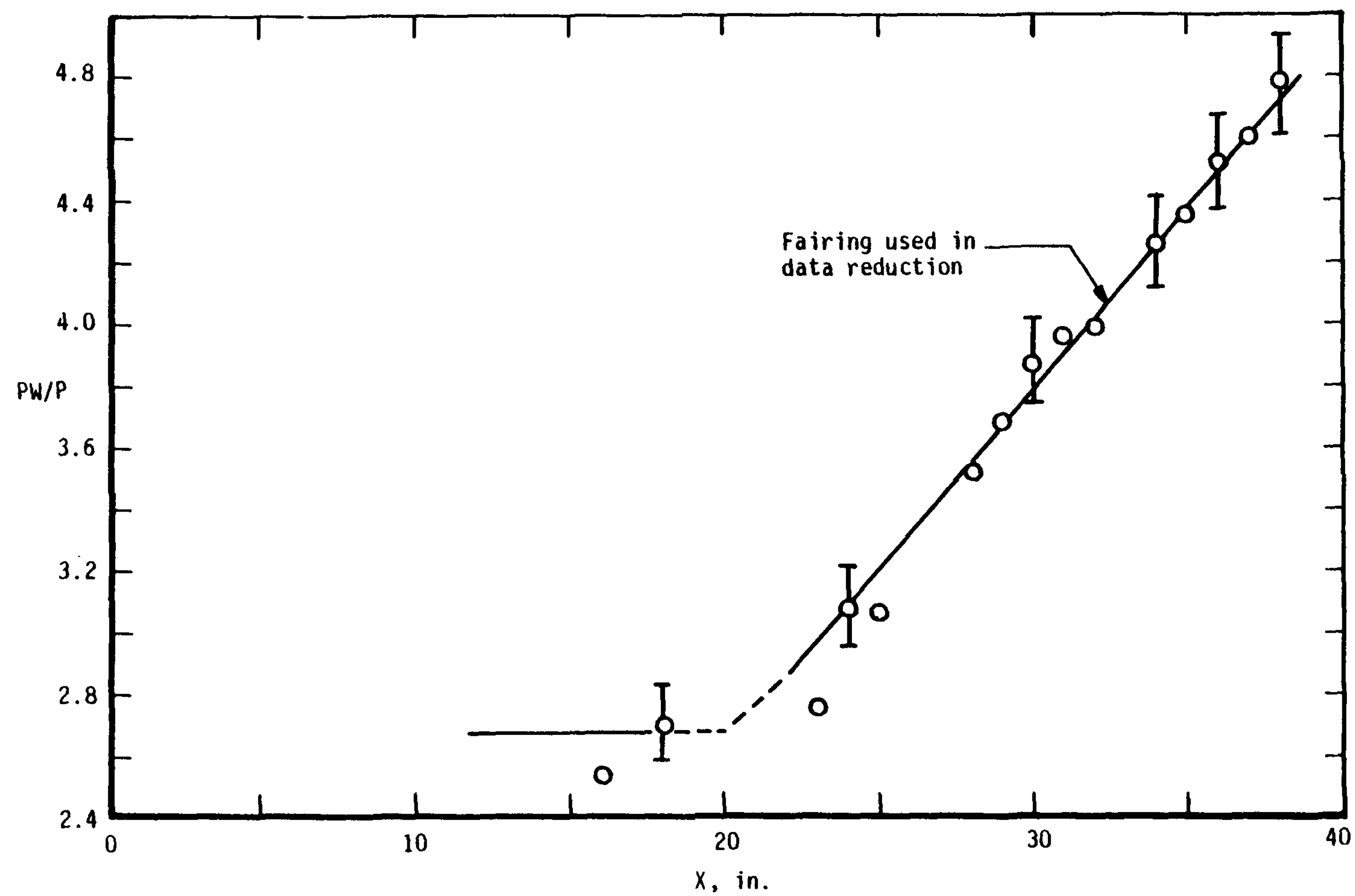

b. Configuration DP/DX : 4

Figure 8. Concluded

TABLE 1. MODEL INSTRUMENTATION LOCATIONS

a. Configuration DP/DX: 1

PRESSURE ORIFICE LOCATIONS			COAXIAL THERMOCOUPLE LOCATIONS		
TAP	X (in.)	THETA (deg)	T/C	X (in.)	THETA (deg)
1	12	180	1	12	90
2	14	180	2	14	90
3	16	180	3	16	90
4	18	180	4	18	90
5	22	180	5	22	90
6	23	180	6	23	90
7	24	180	7	24	90
8	25	180	8	25	90
9	26	180	9	26	90
10	27	180	10	27	90
11	28	180	11	28	90
12	29	180	12	29	90
13	30	180	13	30	90
14	31	180	14	31	90
15	32	180	15	32	90
16	33	180	16	33	90
17	34	180	17	34	90
18	35	180	18	35	90
19	36	180	19	36	90
20	37	180	20	37	90
21	38	180			
22	38	270			
23	38	0			
24	38	90			

TABLE 1. CONCLUDED

b. Configuration DP/DX: 4

PRESSURE ORIFICE LOCATIONS			COAXIAL THERMOCOUPLE LOCATIONS		
TAP	X (in.)	THETA (deg)	T/C	X (in.)	THETA (deg)
1	12	180	1	12	90
2	14	180	2	14	90
3	16	180	3	16	90
4	18	180	4	18	90
5	22	180	5	22	90
6	23	180	6	23	90
7	24	180	7	24	90
8	25	180	8	25	90
9	26	180	9	26	90
10	27	180	10	27	90
11	28	180	11	28	90
12	29	180	12	29	90
13	30	180	13	30	90
14	31	180	14	31	90
15	32	180	15	32	90
16	33	180	16	33	90
17	34	180	17	34	90
18	35	180	18	35	90
19	36	180	19	36	90
20	37	180	20	37	90
21	38	180	21	36	95.75
22	38	270	22	36	101.5
23	38	0	23	36.35	102.1
24	38	90	24	36.70	102.7
			25	37.05	103.3
			26	37.40	103.9
			27	37.75	104.5

TABLE 2. ESTIMATED UNCERTAINTIES OF MEASURED PARAMETERS

Parameter Designation	Steady-State Estimated Measurement*							Range	Type of Measuring Device	Type of Recording Device	Method of System Calibration
	Precision Index (S)			Bias (B)		Uncertainty ± (B + t_{95}S)					
	Percent of Reading	Unit of Measurement	Degree of Freedom	Percent of Reading	Unit of Measurement	Percent of Reading	Unit of Measurement				
Stilling Chamber Pressure (PT), psi		± 0.1 psi	> 30		± 0.1 psi		± 0.3 psi	0 to 900 psi	Paroscientific Digiquartz Pressure Transducer	Digital data acquisition system	In-place application of multiple pressure levels measured with a pressure measuring device *calibrated* in the standards laboratory
Total Temperature (TT), °F		± 1°F ± 1°F	> 30 > 30	± 0.375	± 2°F	± (0.375	± 4°F % + 2°F)	< 530° < 2300°F	Chromel®-Alumel® Thermocouple	Digital Thermometer and Micro Processor *Averaged (TTP) Digital* Thermometer for Redundant (TTR)	Thermocouple verification of NBS *conformity/voltage* substitution calibration
Angle of Attack (ALPHA), deg		± 0.025 deg	> 30		0 ◆		± 0.05 deg	± 15 deg	Potentiometer	Digital data acquisition system/analog-to-digital converter	Heidenhain rotary encorder ROD700 Resolution: 0.0006° Overall accuracy: 0.001°
Roll Angle (PHI), deg		*± 0.15 deg*	*> 30*		0 ◆		± 0.3 deg	± 180 deg	Potentiometer	Digital data acquisition system/analog-to-digital converter	Heidenhain rotary encorder ROD700 Resolution: 0.0006° Overall accuracy: 0.001°
Pitot Pressure (PP), psi		± 0.002 psi			± 0.010 psi		± 0.014 psi	< 10 psid	Druck ± 15 psid strain gage transducers	Analog to digital converter/digital data acquisition system	In-place application of multiple pressure levels measured with a pressure measuring device calibrated in the *standards laboratory*
TTTU, °F		± 1°F ± 1°F	> 30 > 30	± 0.375	± 2°F	± (0.375	± 4°F % + 2°F	< 530 °F < 2300 °F	Unshielded Chromel-Alumel Thermocouple	Analog to digital converter/digital data acquisition system	Thermocouple verification of NBS conformity/voltage substitution calibration

*Reference: Abernethy, R.B. et al and Thompson, J. W. "Handbook Uncertainty in Gas Turbine Measurements." AEDC-TR-73-5, February 1973.

Note: ◆ *Bias assumed to be zero*

TABLE 2. CONCLUDED

Parameter Designation	Steady-State Estimated Measurement*							Range	Type of Measuring Device	Type of Recording Device	Method of System Calibration
	Precision Index (S)			Bias (B)		Uncertainty ±(B + t_{95}S)					
	Percent of Reading	Unit of Measurement	Degree of Freedom	Percent of Reading	Unit of Measurement	Percent of Reading	Unit of Measurement				
Model Pressure (PW), psi		± .00075 psi ± .002 psi ± .002 psi	>30 >30 >30	± 1.0 ± 0.1	± 0.003 psi	± (1% ± (0.1%	+ 0.0015 psi) + 0.004 psi) ± 0.007 psi	0 ≤ P ≤ 0.15 psid 0.15 ≤ P ≤1.5 psid <2.5	Druck ± 1 psid strain gage transducers ESP* 2.5 psid strain gage transducer	Analog to digital converter/digital data acquisition system	In-p ace application of multiple pressure levels measured with a pressure measuring device calibrated in the Standards Lab
Model Temperature (TW), °F		± 1°F ± 1°F	>30 >30	± 0.375	± 2.2°F	± (0.375 %	± 4.2°F + 2°F)	<600°F <1600°F	Iron-Constantan Thermocouple	Digital data acquisition system analog-to-digital converter	Thermocouple verification of NBS conformity/voltage substitution calibration
Probe Height Relative to Model Surface (ZA, ZF, ZP, ZT), in.		± 0.001 in.	>30		± 0.002 in.		± 0.004 in.	<9.0 in.	Potentiometer and Optical	Digital data acquisition system/analog-to-digital converter	Precision Micrometer
Survey Station (XSTA), in.		± 0.011 in.	>30		± 0.012 in.		± 0.034 in.	<26 in.	Potentiometer	Digital data acquisition System A/D Converter Optically Positioned Zero	Precision Micrometer
Heat Transfer Gage Output (E), mv	± 0.1		>30		± 0.01 mv	± (0.2%	+ 0.01.1 mv)	0 to 10 mv	Millivolt source	Analog to digital converter/digital data acquisition system	Millivolt standard referenced to lab standard
Heat Transfer (QDOT), Btu/ft² sec	± 1.5	± 0.015 Btu/ft2-sec	>30 >30	2 2		± (2% + ± 5	0.03 Btu/ft²-sec)	<1 1 to 10 Btu/ft²-sec	Schmidt-Boelter gage	Analog to digital converter/digital data acquisition system	Radiant heat source and secondary standard
ERMSA and ERMSF, mv CURRENT, ma EBAR, mv	± 0.5 ± 0.5 ± 0.5			0⁺ 0⁺ 0⁺		± 1 ± 1 ± 1		<1200 mv <5 ma <300 mv	Philco Ford Corp. Model #ADP-12/13 Hot-wire Anemometer System	Digital data acquisition system/analog-to-digital converter	Precision Digital Voltmeter

*Reference: Abernethy, R.B. et al and Thompson, J. W. "Handbook Uncertainty in Gas Turbine Measurements." AEDC-TR-73-5, February 1973.

Note: + Bias assumed to be zero

TABLE 3. TEST RUN SUMMARY

a. Hot-Wire Anemometer Measurements at Location of Maximum Disturbance Energy in Boundary Layer - Run Summary

CONFIGURATION	NOMINAL X STATION / RUN NUMBERS - RE/FT = 1.0 million																											
	11	12	13	14	15	16	17	18	19	20	21	22	23	24	25	26	27	28	29	30	31	32	33	34	35	36	37	XSTA
DP/DX: 1	140	139	138	137	136	135	134	133	132	131	130	129	128	127	126	125	124	123	122	121	120	119	118	117	116	115	114	RUNS
DP/DX: 4	79	78	77	76	75	74	73	72	71	70	69	68	67	66	65	64	63	62	61	45 60	44	43 80	42	41 81	40	39	38	RUNS

b. Boundary-Layer Profiles - Run Summary

CONFIGURATION	NOMINAL X STATION / RUN NUMBERS - RE/FT = 1.0 million								
	11	15	20	24	28	32	35	36	XSTA
DP/DX: 1	154	152	148 153	149 150	147	145 151		144 146	RUNS
DP/DX: 4			85	88	84	83	86 + 87 89	82	RUNS

TABLE 3. CONTINUED

c. Supplementary Probe Data - Run Summary

RE/FT x 10^{-6}	PROBE CALIBRATION DATA			FREE-STREAM FLUCTUATION DATA		
	SET 1	SET 2	SET 3	SET 1	SET 2	SET 3
0.5	23	56	104	24	57	105
0.8	25, 26	54	106	27	55	107
1.0	29	52	108	30	53	109
1.2	32	50	110	33	51	111
1.5	35	48	112	36	49	113

Probe Identification Numbers

Probe Assembly	Hot-Wire Probe	Hot-Film Probe	Total-Temp. Probe	Pitot Probe
SET 1	3	49	91	81
SET 2	9	58	92	91
SET 3	34	51	92	91

TABLE 3. CONCLUDED

d. Model Surface Data - Run Summary

CONFIGURATION DP/DX: 1

RE/FT x 10^{-6}	Pressure and Temperature Data	Heat-Transfer Data
0.5	--	101, 102, 103
1.0	141, 142, 143, 155, 156*	98, 99, 100
1.5	--	95, 96, 97
2.0	--	92, 93, 94

* PHI = 180 deg

CONFIGURATION DP/DX: 4

RE/FT x 10^{-6}	Pressure and Temperature Data	Heat-Transfer Data
0.5	58	18-22
1.0	28, 37, 59	11-16
1.2	31	--
1.5	34	7-10
2.0	--	1-6

TABLE 4. ESTIMATED UNCERTAINTIES OF CALCULATED PARAMETERS

Parameter Designation	Precision Index (S)			Bias (B)		Uncertainty $\pm(B + t_{95}S)$		RE/FT x 10^{-6} Nom.	MACH, Nominal
	Percent of Reading	Unit of Measurement	Degree of Freedom	Percent of Reading	Unit of Measurement	Percent of Reading	Unit of Measurement		
P, psi	1.03		<30	0.05		2.11		1.0	8.0
PT2, psi	0.70			0.05		1.45			
Q, psi	0.70			0.05		1.45			
T, °F	0.30			0.24		0.85			
V, ft/sec	0.04			0.12		0.21			
RHO, lbm/ft3	0.74			0.25		1.73			
MU, lbf-sec/ft2	0.29			0.44		1.02			
M	0.17 + +			0 +		0.34			
RE/FT	0.57			0.25		1.40			
P, psi	0.52		<30	0.03		1.07		1.5	8.0
PT2, psi	0.35			0.03		0.73			
Q, psi	0.35			0.03		0.73			
T, °F	0.17			0.24		0.58			
V, ft/sec	0.04			0.12		0.20			
RHO, lbm/ft3	0.38			0.25		1.01			
MU, lbf-sec/ft2	0.17			0.41		0.75			
M	0.08 + +			0 +		0.17			
RE/FT	0.30			0.25		0.85			
P, psi	0.52			0.03		1.07		2.0	8.0
PT2, psi	0.35			0.03		0.73			
Q, psi	0.35			0.03		0.73			
T, °F	0.17			0.24		0.58			
V, ft/sec	0.04			0.12		0.20			
RHO, lbm/ft3	0.38			0.25		1.01			
MU, lbf-sec/ft2	0.16			0.40		0.72			
M	0.08 + +			0 +		0.17			
RE/FT	0.30			0.25		0.85			

NOTE: + Bias assumed to be zero

+ + Determined from test section repeatability and uniformity during tunnel calibration

DATE COMPUTED 9-MAY-90
DATE RECORDED 9-MAY-90
TIME RECORDED 3:24: 49
TIME COMPUTED 03:27:08
PROJECT NUMBER CP91VB

HYPERSONIC BOUNDARY LAYER STABILITY

RUN NUMBER 60 PAGE 1

CONFIG: PRESSURE GRADIENT DP/DX: 4 (RN = 0.002 IN.)
XSTA = 30.00 IN.

DATA TYPE 9
HOT WIRE ANEMOMETER DATA

POINT	CURRENT (MAMP)	EBAR (MV)	ERMSA (MV)	R (OHM)	POWER	PT (PSIA)	TT (DEG R)	Q (PSIA)	RE (PER IN)	ZA (IN.)
1	0.002	0.28	110.03	96.184	3.752E+00	2.250E+02	1.303E+03	1.061E+00	8.427E+04	9.695E-02
2	0.199	20.51	116.18	0.000	0.000E+00	2.249E+02	1.304E+03	1.061E+00	8.413E+04	9.768E-02
3	0.403	41.75	133.82	100.583	4.199E+00	2.250E+02	1.304E+03	1.061E+00	8.417E+04	9.548E-02
4	0.616	63.74	161.76	100.436	1.742E+01	2.251E+02	1.304E+03	1.061E+00	8.420E+04	9.842E-02
5	0.801	83.48	194.29	101.272	3.669E+01	2.253E+02	1.304E+03	1.062E+00	8.428E+04	9.842E-02
6	0.999	104.17	236.94	101.228	6.477E+01	2.253E+02	1.304E+03	1.062E+00	8.428E+04	9.768E-02
7	1.198	126.29	292.27	102.531	1.023E+02	2.253E+02	1.304E+03	1.062E+00	8.428E+04	9.768E-02
8	1.401	148.95	360.96	103.511	1.495E+02	2.253E+02	1.304E+03	1.062E+00	8.428E+04	9.548E-02
9	1.555	166.75	425.06	104.525	1.921E+02	2.253E+02	1.304E+03	1.062E+00	8.428E+04	9.695E-02
10	1.694	183.18	491.82	105.442	2.357E+02	2.251E+02	1.304E+03	1.061E+00	8.420E+04	9.768E-02
11	1.849	202.19	579.21	106.739	2.906E+02	2.250E+02	1.304E+03	1.061E+00	8.417E+04	9.622E-02
12	2.012	222.77	688.66	108.232	3.556E+02	2.250E+02	1.304E+03	1.061E+00	8.417E+04	9.695E-02

ALPHA = 0.03 DEG XC 30.27 (IN)

MACH 7.93

C1W = 100.204 C2W = 0.022400

PT = 225.04 PSIA P = 2.408E-02 PSIA
TT =1302.67 DEGR T = 9.769E+01 DEGR

RUN 60

<u>Note</u>: Gain for ERMSA is 200.

Sample 1. Anemometer Data

HYPERSONIC BOUNDARY LAYER STABILITY

RUN NUMBER 60 PAGE 2

DATE COMPUTED 9-MAY-90
DATE RECORDED 9-MAY-90
TIME RECORDED 3:24: 49
TIME COMPUTED 03:27:08
PROJECT NUMBER CP91VB

CONFIG: PRESSURE GRADIENT DP/DX: 4 (RN = 0.002 IN.)
XSTA = 30.00 IN.

DATA TYPE 9
HOT FILM ANEMOMETER DATA

POINT	CURRENT (MAMP)	EBAR (MV)	ERMSF (MV)	R (OHM)	POWER	PT (PSIA)	TT (DEG R)	Q (PSIA)	RE (PER IN)	ZF (IN.)
1	0.002	0.02	182.97	20.949	1.223E+03	2.250E+02	1.303E+03	1.061E+00	8.427E+04	1.008E 01
2	7.600	193.82	207.58	0.000	0.000E+00	2.249E+02	1.304E+03	1.061E+00	8.413E+04	1.015E-01
3	18.945	487.03	318.22	22.485	2.894E+03	2.250E+02	1.304E+03	1.061E+00	8.417E+04	9.933E-02
4	30.225	791.43	442.44	23.054	1.189E+04	2.251E+02	1.304E+03	1.061E+00	8.420E+04	1.023E-01
5	41.421	1110.70	561.04	23.750	2.717E+04	2.253E+02	1.304E+03	1.062E+00	8.428E+04	1.023E-01
6	50.656	1390.56	649.96	24.435	4.530E+04	2.253E+02	1.304E+03	1.062E+00	8.428E+04	1.015E-01
7	57.975	1627.12	718.31	25.092	6.368E+04	2.253E+02	1.304E+03	1.062E+00	8.428E+04	1.015E-01
8	65.228	1874.47	787.86	25.804	8.569E+04	2.253E+02	1.304E+03	1.062E+00	8.428E+04	9.933E-02
9	70.639	2068.02	852.65	26.371	1.048E+05	2.253E+02	1.304E+03	1.062E+00	8.428E+04	1.008E-01
10	74.480	2158.34	870.87	26.014	1.164E+05	2.251E+02	1.304E+03	1.061E+00	8.420E+04	1.015E-01
11	78.166	2274.66	908.39	26.128	1.301E+05	2.250E+02	1.304E+03	1.061E+00	8.417E+04	1.001E-01
12	81.695	2413.76	953.61	26.600	1.460E+05	2.250E+02	1.304E+03	1.061E+00	8.417E+04	1.008E-01

ALPHA = 0.03 DEG XC 30.27 (IN)

MACH 7.93

C1F = 22.933 C2F = 0.000028

PT = 225.04 PSIA P = 2.408E-02 PSIA
TT =1302.67 DEGR T = 9.769E+01 DEGR

RUN 60

Note: Gain for ERMSF is 50.

Sample 1. Concluded

DATE COMPUTED	9-MAY-90
DATE RECORDED	9-MAY-90
TIME RECORDED	2:16: 8
TIME COMPUTED	02:16:34
PROJECT NUMBER	CP91VB

HYPERSONIC BOUNDARY LAYER STABILITY

RUN NUMBER 52 PAGE 1

CONFIG: PRESSURE GRADIENT DP/DX: 4 (RN = 0.002 IN.)
XSTA = 37.00 IN.

DATA TYPE 6 PROBE FLOW CALIBRATION

POINT	M	PT (PSIA)	TT (DEG R)	RE (PER FT)	PP (PSIA)	ML	TTTU (DEG R)	TTTU/TT	ETA	RETD**.5
1	7.932	223.44	1310.67	9.943E+05	1.9626	7.9394	1202.6700	0.9176	0.9109	6.778E+00

RUN 52

Sample 2. Probe Flow Calibration Data

HYPERSONIC BOUNDARY LAYER STABILITY

RUN NUMBER 83 PAGE 1

DATE COMPUTED 4-JUN-90
DATE RECORDED 9-MAY-90
TIME RECORDED 6:21: 40
TIME COMPUTED 06:35:49
PROJECT NUMBER CP91VB

CONFIG: PRESSURE GRADIENT DP/DX: 4 (RN = 0.002 IN.)
XSTA = 32.00 IN.

DATA TYPE 4
FLOW FIELD SURVEYS

POINT	PT (PSIA)	TT (DEG R)	PT2 (PSIA)	P (PSIA)	ZP (IN)	PP (PSIA)	PWL (PSIA)	TWL (DEG R)	ZT (IN)	TTTU (DEGR)	ZA (IN)	E RMSA (MV RMS)	ZF (IN)	E RMSF (MV RMS)
1	224.84	1307.7	1.968	0.024	0.0458	0.1620	0.101	1146.2	0.0656	1136.7	0.0835	131.836	0.0754	158.6914
2	225.35	1307.7	1.972	0.024	0.0488	0.1731	0.102	1146.1	0.0685	1137.7	0.0865	131.836	0.0783	200.8057
3	225.14	1307.7	1.970	0.024	0.0539	0.1881	0.101	1146.1	0.0737	1138.7	0.0916	131.836	0.0835	219.7268
4	225.14	1307.7	1.970	0.024	0.0590	0.2071	0.101	1146.5	0.0788	1140.7	0.0967	130.615	0.0886	238.6475
5	225.34	1307.7	1.972	0.024	0.0627	0.2391	0.102	1146.4	0.0825	1143.7	0.1004	131.226	0.0923	279.5410
6	225.54	1307.7	1.974	0.024	0.0693	0.2791	0.102	1146.4	0.0891	1150.7	0.1070	130.615	0.0989	349.1211
7	225.74	1308.7	1.975	0.024	0.0752	0.3331	0.102	1146.3	0.0950	1158.7	0.1128	131.226	0.1048	427.2461
8	225.65	1308.7	1.974	0.024	0.0774	0.4061	0.102	1146.4	0.0972	1169.7	0.1150	131.226	0.1070	499.2676
9	225.64	1308.7	1.974	0.024	0.0854	0.5072	0.102	1146.6	0.1052	1183.7	0.1231	130.615	0.1150	557.2510
10	225.44	1308.7	1.973	0.024	0.0884	0.6372	0.102	1146.4	0.1082	1199.7	0.1260	131.226	0.1180	596.3135
11	225.25	1308.7	1.971	0.024	0.0950	0.8122	0.102	1147.0	0.1148	1212.7	0.1326	131.226	0.1246	632.9346
12	225.04	1308.7	1.969	0.024	0.0979	1.0493	0.101	1146.8	0.1177	1225.7	0.1356	130.005	0.1275	666.5039
13	224.74	1308.7	1.967	0.024	0.1045	1.3224	0.101	1146.5	0.1243	1235.7	0.1422	130.005	0.1341	704.9561
14	224.84	1309.7	1.968	0.024	0.1111	1.6095	0.101	1146.5	0.1309	1242.7	0.1487	130.615	0.1407	737.9150
15	225.04	1309.7	1.969	0.024	0.1141	1.9206	0.101	1147.0	0.1339	1244.7	0.1517	130.615	0.1437	755.0049
16	225.15	1309.7	1.970	0.024	0.1192	2.2047	0.101	1146.6	0.1390	1244.7	0.1568	131.226	0.1488	740.3564
17	225.14	1309.7	1.970	0.024	0.1236	2.4787	0.101	1146.7	0.1434	1243.7	0.1612	131.226	0.1532	704.9561
18	224.94	1310.7	1.968	0.024	0.1302	2.7948	0.101	1146.7	0.1500	1241.7	0.1678	130.005	0.1598	653.6865
19	224.84	1310.7	1.968	0.024	0.1361	3.1249	0.101	1147.0	0.1559	1237.7	0.1737	130.005	0.1657	590.2100
20	225.24	1310.7	1.971	0.024	0.1375	3.5131	0.102	1146.8	0.1574	1235.7	0.1751	130.005	0.1671	513.3057
21	225.35	1310.7	1.972	0.024	0.1456	3.8752	0.102	1146.9	0.1654	1233.7	0.1832	130.615	0.1752	444.9463
22	225.24	1310.7	1.971	0.024	0.1493	4.2393	0.102	1147.2	0.1691	1231.7	0.1869	130.615	0.1789	381.4697
23	225.15	1311.7	1.970	0.024	0.1559	4.5494	0.101	1147.3	0.1757	1230.7	0.1935	130.005	0.1855	326.5381
24	225.14	1311.7	1.970	0.024	0.1588	4.7894	0.101	1147.4	0.1787	1229.7	0.1964	130.005	0.1884	282.5928
25	225.24	1311.7	1.971	0.024	0.1647	4.9665	0.102	1147.1	0.1845	1229.7	0.2023	130.005	0.1943	250.8545
26	225.14	1311.7	1.970	0.024	0.1698	5.0835	0.101	1147.2	0.1897	1229.7	0.2074	120.850	0.1994	236.2061
27	225.35	1311.7	1.972	0.024	0.1757	5.1655	0.102	1147.6	0.1955	1229.7	0.2132	120.239	0.2053	222.7783
28	225.35	1312.7	1.972	0.024	0.1808	5.2076	0.102	1147.6	0.2007	1229.7	0.2184	119.629	0.2104	205.6885
29	225.34	1312.7	1.972	0.024	0.1852	5.2186	0.102	1147.3	0.2051	1229.7	0.2228	120.239	0.2148	223.3887
30	224.95	1312.7	1.968	0.024	0.1874	5.2136	0.101	1147.4	0.2073	1229.7	0.2250	120.850	0.2170	154.4189
31	224.74	1312.7	1.967	0.024	0.1955	5.2096	0.101	1147.8	0.2154	1229.7	0.2330	119.629	0.2251	156.2500
32	225.24	1312.7	1.971	0.024	0.1999	5.2206	0.102	1147.9	0.2198	1230.7	0.2374	119.629	0.2295	151.9775
33	225.55	1312.7	1.973	0.024	0.2036	5.2196	0.102	1147.9	0.2234	1230.7	0.2411	120.239	0.2332	149.5361
34	225.75	1313.7	1.975	0.024	0.2102	5.2136	0.102	1147.8	0.2300	1230.7	0.2477	120.239	0.2398	153.8086
35	225.54	1313.7	1.973	0.024	0.2168	5.2006	0.102	1148.1	0.2366	1230.7	0.2543	120.239	0.2464	164.1846
36	225.44	1313.7	1.97[illegible]	0.024	0.2175	5.1916	0.102	1147.7	0.2374	1230.7	0.2550	119.019	0.2471	151.3672
37	225.45	1313.7	1.973	0.024	0.2249	5.1836	0.102	1148.1	0.2447	1230.7	0.2624	120.239	0.2545	149.5361
38	225.25	1313.7	1.971	0.024	0.2315	5.1756	0.102	1147.8	0.2513	1230.7	0.2690	120.850	0.2611	153.8086
39	224.94	1313.7	1.968	0.024	0.2351	5.1575	0.101	1147.9	0.2550	1230.7	0.2726	120.850	0.2647	151.9775
40	224.85	1313.7	1.967	0.024	0.2388	5.1605	0.101	1148.2	0.2587	1230.7	0.2763	119.629	0.2684	150.7568

Sample 3. Flow-Field Survey Data

RUN NUMBER 83 PAGE 2

DATA TYPE 4
FLOW FIELD SURVEYS

POINT	PT (PSIA)	TT (DEG R)	PT2 (PSIA)	P (PSIA)	ZP (IN)	PP (PSIA)	PWL (PSIA)	TWL (DEG R)	ZT (IN)	TTTU (DEGR)	ZA (IN)	RMSA (MV RMS)	ZF	RMSF
41	224.94	1313.7	1.968	0.024	0.2447	5.1585	0.101	1148.2	0.2645	1231.7	0.2821	119.629	0.2743	147.0947
42	225.04	1313.7	1.969	0.024	0.2498	5.1585	0.101	1148.0	0.2697	1231.7	0.2873	119.629	0.2794	153.1982
43	225.34	1313.7	1.972	0.024	0.2557	5.1555	0.102	1148.1	0.2756	1231.7	0.2931	120.239	0.2853	154.4189
44	225.35	1313.7	1.972	0.024	0.2586	5.1505	0.102	1148.2	0.2785	1231.7	0.2961	120.239	0.2882	151.3672
45	225.35	1313.7	1.972	0.024	0.2660	5.1485	0.102	1148.1	0.2858	1231.7	0.3034	120.239	0.2956	147.7051
46	225.14	1313.7	1.970	0.024	0.2711	5.1365	0.101	1148.4	0.2910	1231.7	0.3085	120.239	0.3007	153.8086

MEAN VALUES

PHI = 0.01

M = 7.93
ALPHA = 0.0 DEG
DEW = -60. DEG R

XC = 32.1139

PT =	225.2	PSIA
TT =	1311.1	DEG R
PT2 =	1.971	PSIA
RE =	1.002E+06	PER FT
MU =	7.916E-08	LBF-SEC/FT2
RHO =	6.613E-04	LBM/FT3

P =	0.0241	PSIA
PWL =	0.1015	PSIA
TWL =	1147.2	DEG R
V =	3857.1	FT/SEC
Q =	1.062	PSIA
T =	98.4	DEG R

Sample 3. Continued

DATE COMPUTED 4-JUN-90
DATE RECORDED 9-MAY-90
TIME RECORDED 6:21: 40
TIME COMPUTED 06:35:50
PROJECT NUMBER CP91VB

HYPERSONIC BOUNDARY LAYER STABILITY

RUN NUMBER 83 PAGE 3

CONFIG: PRESSURE GRADIENT DP/DX: 4 (RN = 0.002 IN.)
XSTA = 32.00 IN.

DATA TYPE 4
FLOW FIELD SURVEYS

	ZP (IN)	PP/PPE	ML	ML/ME	TTLU (DEG R)	TTL (DEG R)	TTL/TTE	TL (DEG R)	UL (FT/SEC)	UL/UE	LRE (PER IN)	LRET (PER IN)
1	0.0458	0.032	8.47E-01	0.136	1139.5	1153.9	0.881	1009.1	1.319E+03	0.353	1.537E+03	1.408E+03
2	0.0488	0.034	9.07E-01	0.145	1139.1	1155.2	0.882	992.1	1.400E+03	0.375	1.682E+03	1.522E+03
3	0.0539	0.037	9.82E-01	0.157	1138.4	1156.7	0.883	969.8	1.499E+03	0.401	1.868E+03	1.664E+03
4	0.0590	0.040	1.06E+00	0.170	1137.6	1158.5	0.884	944.9	1.602E+03	0.429	2.088E+03	1.824E+03
5	0.0627	0.047	1.18E+00	0.189	1137.1	1161.7	0.886	908.2	1.745E+03	0.467	2.431E+03	2.065E+03
6	0.0693	0.054	1.31E+00	0.210	1137.8	1166.5	0.890	868.5	1.892E+03	0.507	2.844E+03	2.337E+03
7	0.0752	0.065	1.46E+00	0.234	1139.3	1172.8	0.895	821.3	2.055E+03	0.550	3.397E+03	2.677E+03
8	0.0774	0.079	1.65E+00	0.264	1140.1	1179.2	0.900	764.8	2.231E+03	0.597	4.161E+03	3.109E+03
9	0.0854	0.099	1.87E+00	0.299	1146.8	1192.4	0.910	702.4	2.427E+03	0.650	5.237E+03	3.655E+03
10	0.0884	0.124	2.12E+00	0.340	1149.9	1202.1	0.917	633.2	2.615E+03	0.700	6.746E+03	4.342E+03
11	0.0950	0.158	2.42E+00	0.387	1158.8	1217.9	0.929	561.7	2.808E+03	0.752	8.926E+03	5.209E+03
12	0.0979	0.204	2.77E+00	0.444	1171.0	1237.0	0.944	488.3	2.999E+03	0.803	1.221E+04	6.331E+03
13	0.1045	0.257	3.13E+00	0.501	1182.4	1253.9	0.957	424.4	3.157E+03	0.845	1.653E+04	7.591E+03
14	0.1111	0.313	3.46E+00	0.554	1205.5	1281.8	0.978	377.7	3.296E+03	0.882	2.138E+04	8.786E+03
15	0.1141	0.374	3.79E+00	0.607	1211.3	1290.3	0.985	333.5	3.391E+03	0.908	2.774E+04	1.020E+04
16	0.1192	0.429	4.06E+00	0.651	1227.9	1309.5	0.999	304.4	3.475E+03	0.930	3.380E+04	1.136E+04
17	0.1236	0.483	4.31E+00	0.691	1234.6	1317.4	1.005	279.0	3.532E+03	0.946	4.055E+04	1.254E+04
18	0.1302	0.544	4.59E+00	0.735	1241.9	1325.7	1.012	254.5	3.588E+03	0.960	4.913E+04	1.390E+04
19	0.1361	0.608	4.86E+00	0.778	1244.7	1328.7	1.014	232.4	3.629E+03	0.972	5.930E+04	1.537E+04
20	0.1375	0.684	5.15E+00	0.825	1244.7	1328.3	1.014	210.7	3.664E+03	0.981	7.277E+04	1.715E+04
21	0.1456	0.754	5.41E+00	0.867	1243.0	1325.9	1.012	193.4	3.689E+03	0.987	8.699E+04	1.884E+04
22	0.1493	0.825	5.66E+00	0.907	1241.9	1323.9	1.010	178.6	3.710E+03	0.993	1.026E+05	2.053E+04
23	0.1559	0.886	5.87E+00	0.941	1237.7	1318.6	1.006	167.1	3.720E+03	0.996	1.175E+05	2.205E+04
24	0 1588	0.932	6.02E+00	0.965	1235.3	1315.4	1.004	159.3	3.727E+03	0.998	1.295E+05	2.321E+04
25	0 1647	0.967	6.13E+00	0.983	1233.9	1313.3	1.002	154.0	3.732E+03	0.999	1.388E+05	2.407E+04
26	0.1698	0.990	6.21E+00	0.995	1231.6	1310.5	1.000	150.5	3.733E+03	0.999	1.454E+05	2.467E+04
27	0.1757	1.006	6.26E+00	1.002	1230.7	1309.3	0.999	148.3	3.735E+03	1.000	1.498E+05	2.507E+04
28	0.1808	1.014	6.28E+00	1.007	1229.7	1308.1	0.998	147.1	3.735E+03	1.000	1.523E+05	2.529E+04
29	0.1852	1.016	6.29E+00	1.008	1229.7	1308.0	0.998	146.8	3.735E+03	1.000	1.529E+05	2.534E+04
30	0.1874	1.015	6.29E+00	1.008	1229.7	1308.1	0.998	146.7	3.736E+03	1.000	1.528E+05	2.532E+04
31	0.1955	1.014	6.29E+00	1.008	1229.7	1308.1	0.998	146.7	3.736E+03	1.000	1.527E+05	2.530E+04
32	0.1999	1.016	6.29E+00	1.008	1229.7	1308.0	0.998	146.7	3.736E+03	1.000	1.531E+05	2.535E+04
33	0.2036	1.016	6.29E+00	1.007	1229.7	1308.0	0.998	146.9	3.735E+03	1.000	1.528E+05	2.535E+04
34	0.2102	1.015	6.28E+00	1.006	1229.7	1308.0	0.998	147.2	3.735E+03	1.000	1.524E+05	2.532E+04
35	0.2168	1.012	6.27E+00	1.005	1230.0	1308.4	0.998	147.4	3.735E+03	1.000	1.517E+05	2.525E+04
36	0.2175	1.011	6.27E+00	1.005	1230.2	1308.6	0.999	147.6	3.735E+03	1.000	1.513E+05	2.521E+04
37	0.2249	1.009	6.27E+00	1.004	1230.7	1309.2	0.999	147.9	3.736E+03	1.000	1.507E+05	2.516E+04
38	0.2315	1.008	6.26E+00	1.004	1230.7	1309.2	0.999	148.0	3.735E+03	1.000	1.504E+05	2.512E+04
39	0.2351	1.004	6.26E+00	1.002	1230.7	1309.3	0.999	148.3	3.735E+03	1.000	1.496E+05	2.503E+04
40	0.2388	1.005	6.26E+00	1.003	1230.7	1309.3	0.999	148.2	3.735E+03	1.000	1.498E+05	2.505E+04
41	0.2447	1.004	6.26E+00	1.003	1230.7	1309.3	0.999	148.3	3.735E+03	1.000	1.497E+05	2.504E+04
42	0.2498	1.004	6.26E+00	1.002	1230.7	1309.3	0.999	148.3	3.735E+03	1.000	1.496E+05	2.504E+04

Sample 3. Continued

RUN NUMBER 83 PAGE 4

DATA TYPE 4
FLOW FIELD SURVEYS

	ZP (IN)	PP/PPE	ML	ML/ME	TTLU (DEG R)	TTL (DEG R)	TTL/TTE	TL (DEG R)	UL (FT/SEC)	UL/UE	LRE (PER IN)	LRET (PER IN)
43	0.2557	1.004	6.25E+00	1.001	1230.7	1309.3	0.999	148.6	3.735E+03	1.000	1.493E+05	2.503E+04
44	0.2586	1.003	6.25E+00	1.001	1230.7	1309.3	0.999	148.7	3.734E+03	1.000	1.490E+05	2.500E+04
45	0.2660	1.002	6.25E+00	1.001	1231.7	1310.4	1.000	148.9	3.736E+03	1.000	1.487E+05	2.497E+04
46	0.2711	1.000	6.24E+00	1.000	1231.7	1310.4	1.000	149.1	3.736E+03	1.000	1.482E+05	2.491E+04

M = 7.93
ALPHA= 0.0 DEG

PHI = 0.01

MEAN VALUES

PT = 225.2 PSIA
TT =1311.1 DEG R
P = 0.0241 PSIA
T = 98.4 DEG R
PT2 = 1.971 PSIA
V = 3857.1 FT/SEC

TWL/TTE = 0.8754
PWL = 0.102 PSIA
TWL =1147.2 DEG R

EDGE VALUES

PPE = 5.137E+00 PSIA
ME = 6.241E+00
TTE = 1.310E+03 DEG R
UE = 0.374E+04 FT/SEC

Sample 3. Continued

HYPERSONIC BOUNDARY LAYER STABILITY

DATE COMPUTED	4-JUN-90
DATE RECORDED	9-MAY-90
TIME RECORDED	6:21: 40
TIME COMPUTED	06:35:50
PROJECT NUMBER	CP91VB

RUN NUMBER 83 PAGE 5

CONFIG: PRESSURE GRADIENT DP/DX: 4 (RN = 0.002 IN.)
XSTA = 32.00 IN.

DATA TYPE 4
MODEL SURFACE MEASUREMENTS

TAP	X (IN)	THETA (DEG)	PW (PSIA)	PW/P
1	12.0	180	0.0816	3.3871
2	14.0	180	0.0725	3.0084
3	16.0	180	0.0612	2.5372
4	18.0	180	0.0654	2.7117
5	22.0	180	0.0747	3.0977
6	23.0	180	0.0665	2.7599
7	24.0	180	0.0746	3.0936
8	25.0	180	0.0739	3.0660
9	26.0	180	0.0596	2.4733
10	27.0	180	0.0882	3.6594
11	28.0	180	0.0849	3.5216
12	29.0	180	0.0889	3.6863
13	30.0	180	0.0935	3.8784
14	31.0	180	0.0954	3.9560
15	32.0	180	0.0960	3.9818
16	33.0	180	0.0890	3.6912
17	34.0	180	0.1027	4.2612
18	35.0	180	0.1048	4.3490
19	36.0	180	0.1092	4.5301
20	37.0	180	0.1109	4.5999
21	38.0	180	0.1155	4.7930
22	38.0	270	0.1267	5.2571
23	38.0	0	0.1191	4.9427
24	38.0	90	0.1124	4.6613

T/C	X (IN)	THETA (DEG)	TW (DEG R)	TW/TT
1	12.00	90.00	1089.9	0.833
2	14.00	90.00	1018.7	0.779
3	16.00	90.00	1019.3	0.779
4	18.00	90.00	1023.3	0.783
5	22.00	90.00	1046.1	0.800
6	23.00	90.00	1055.3	0.807
7	24.00	90.00	1064.5	0.814
8	25.00	90.00	1080.8	0.827
9	26.00	90.00	1092.1	0.835
10	27.00	90.00	1111.9	0.850
11	28.00	90.00	1124.1	0.860
12	29.00	90.00	1133.0	0.866
13	30.00	90.00	1144.8	0.875
14	31.00	90.00	1146.6	0.877
15	32.00	90.00	1147.2	0.877
16	33.00	90.00	1137.2	0.870
17	34.00	90.00	1125.8	0.861
18	35.00	90.00	1112.4	0.851
19	36.00	90.00	1045.2	0.799
20	37.00	90.00	1075.6	0.823
21	36.00	95.75	1094.1	0.837
22	36.00	101.50	1095.8	0.838
23	36.35	102.10	1087.2	0.831
24	36.70	102.70	1081.6	0.827
25	37.05	103.30	1076.9	0.824
26	37.40	103.90	1064.5	0.814
27	37.75	104.50	1056.4	0.808

ALPHA = 0.0 DEG
PHI = 0.0 DEG

XC = 32.114

PT = 225.2 PSIA
TT = 1311.1 DEG R
M = 7.933
RE = 0.100E+07 /FT

TDRK = 564.7 DEG R
P = 0.0241 PSIA
T = 98.3726 DEG R

RUN 83

Sample 3. Continued

HYPERSONIC BOUNDARY LAYER STABILITY

RUN NUMBER 83 PAGE 6

DATE COMPUTED 4-JUN-90
DATE RECORDED 9-MAY-90
TIME RECORDED 6:21: 40
TIME COMPUTED 06:35:51
PROJECT NUMBER CP91VB

CONFIG: PRESSURE GRADIENT DP/DX: 4 (RN = 0.002 IN.)
XSTA = 32.00 IN.

DATA TYPE 4
INTEGRAL EVALUATION

	ZP/DEL	PP/PPD	ML/MD	TTL/TTD	TL/TD	RHOL/RHOD	UL/UD	MUTL/MUTD	LRE/LRED	DITTL/DITTD	LRET/LRETD
1	2.811E-01	3.294E-[illegible]	1.387E-01	8.781E-01	6.493E+00	1.537E-01	3.535E-01	4.818E+00	1.128E-02	4.575E-02	5.905E-02
2	2.991E-01	3.517E-[illegible]	1.485E-01	8.791E-01	6.384E+00	1.567E-01	3.753E-01	4.764E+00	1.234E-02	5.428E-02	6.385E-02
3	3.306E-01	3.822E-02	1.608E-01	8.803E-01	6.240E+00	1.602E-01	4.017E-01	4.692E+00	1.371E-02	6.323E-02	6.979E-02
4	3.621E-01	4.208E-02	1.741E-01	8.816E-01	6.080E+00	1.644E-01	4.294E-01	4.611E+00	1.531E-02	7.148E-02	7.651E-02
5	3.846E-01	4.859E-02	1.935E-01	8.841E-01	5.844E+00	1.712E-01	4.678E-01	4.489E+00	1.784E-02	9.088E-02	8.662E-02
6	4.252E-01	5.672E-02	2.145E-01	8.877E-01	5.588E+00	1.792E-01	5.072E-01	4.354E+00	2.087E-02	1.198E-01	9.804E-02
7	4.612E-01	6.770E-02	2.396E-01	8.925E-01	5.285E+00	1.896E-01	5.507E-01	4.189E+00	2.492E-02	1.576E-01	1.123E-01
8	4.747E-01	8.254E-02	2.696E-01	8.974E-01	4.922E+00	2.035E-01	5.980E-01	3.985E+00	3.054E-02	1.954E-01	1.304E-01
9	5.242E-01	1.031E-01	3.059E-01	9.075E-01	4.520E+00	2.216E-01	6.504E-01	3.750E+00	3.843E-02	2.729E-01	1.533E-01
10	5.422E-01	1.295E-01	3.471E-01	9.148E-01	4.074E+00	2.456E-01	7.007E-01	3.477E+00	4.950E-02	3.319E-01	1.822E-01
11	5.827E-01	1.651E-01	3.958E-01	9.268E-01	3.614E+00	2.766E-01	7.525E-01	3.178E+00	6.550E-02	4.227E-01	2.185E-01
12	6.007E-01	2.133E-01	4.534E-01	9.414E-01	3.142E+00	3.179E-01	8.038E-01	2.852E+00	8.961E-02	5.380E-01	2.656E-01
13	6.412E-01	2.688E-01	5.120E-01	9.543E-01	2.731E+00	3.653E-01	8.461E-01	2.548E+00	1.213E-01	6.414E-01	3.184E-01
14	6.818E-01	3.271E-01	5.666E-01	9.755E-01	2.430E+00	4.107E-01	8.834E-01	2.312E+00	1.569E-01	8.094E-01	3.686E-01
15	6.998E-01	3.904E-01	6.202E-01	9.819E-01	2.146E+00	4.655E-01	9.087E-01	2.078E+00	2.035E-01	8.574E-01	4.279E-01
16	7.313E-01	4.481E-01	6.655E-01	9.965E-01	1.959E+00	5.103E-01	9.314E-01	1.916E+00	2.480E-01	9.754E-01	4.764E-01
17	7.583E-01	5.038E-01	7.065E-01	1.003E+00	1.795E+00	5.567E-01	9.467E-01	1.771E+00	2.975E-01	1.022E+00	5.262E-01
18	7.988E-01	5.680E-01	7.514E-01	1.009E+00	1.638E+00	6.099E-01	9.615E-01	1.626E+00	3.605E-01	1.073E+00	5.832E-01
19	8.348E-01	6.351E-01	7.954E-01	1.011E+00	1.495E+00	6.675E-01	9.727E-01	1.492E+00	4.351E-01	1.089E+00	6.448E-01
20	8.438E-01	7.140E-01	8.434E-01	1.011E+00	1.356E+00	7.374E-01	9.821E-01	1.356E+00	5.340E-01	1.088E+00	7.193E-01
21	8.934E-01	7.876E-01	8.861E-01	1.009E+00	1.245E+00	8.037E-01	9.886E-01	1.245E+00	6.383E-01	1.073E+00	7.901E-01
22	9.159E-01	8.616E-01	9.275E-01	1.008E+00	1.149E+00	8.703E-01	9.943E-01	1.149E+00	7.529E-01	1.059E+00	8.612E-01
23	9.564E-01	9.246E-01	9.614E-01	1.003E+00	1.075E+00	9.297E-01	9.969E-01	1.075E+00	8.619E-01	1.027E+00	9.248E-01
24	9.744E-01	9.734E-01	9.867E-01	1.001E+00	1.025E+00	9.753E-01	9.989E-01	1.025E+00	9.505E-01	1.006E+00	9.736E-01
25	1.010E+00	1.009E+00	1.005E+00	9.994E-01	9.911E-01	1.009E+00	1.000E+00	9.911E-01	1.018E+00	9.959E-01	1.010E+00
26	1.042E+00	1.033E+00	1.017E+00	9.973E-01	9.682E-01	1.032E+00	1.001E+00	9.682E-01	1.067E+00	9.780E-01	1.035E+00
27	1.078E+00	1.050E+00	1.025E+00	9.964E-01	9.543E-01	1.048E+00	1.001E+00	9.543E-01	1.099E+00	9.683E-01	1.052E+00
28	1.109E+00	1.058E+00	1.029E+00	9.955E-01	9.466E-01	1.057E+00	1.001E+00	9.466E-01	1.118E+00	9.613E-01	1.061E+00
29	1.136E+00	1.061E+00	1.030E+00	9.954E-01	9.448E-01	1.059E+00	1.001E+00	9.448E-01	1.122E+00	9.626E-01	1.063E+00
30	1.150E+00	1.060E+00	1.030E+00	9.955E-01	9.442E-01	1.058E+00	1.001E+00	9.442E-01	1.122E+00	9.625E-01	1.062E+00
31	1.199E+00	1.059E+00	1.030E+00	9.955E-01	9.441E-01	1.057E+00	1.001E+00	9.441E-01	1.121E+00	9.603E-01	1.061E+00
32	1.226E+00	1.061E+00	1.030E+00	9.954E-01	9.441E-01	1.059E+00	1.001E+00	9.441E-01	1.123E+00	9.590E-01	1.064E+00
33	1.249E+00	1.061E+00	1.030E+00	9.954E-01	9.453E-01	1.059E+00	1.001E+00	9.453E-01	1.122E+00	9.592E-01	1.063E+00
34	1.290E+00	1.060E+00	1.029E+00	9.954E-01	9.470E-01	1.058E+00	1.001E+00	9.470E-01	1.118E+00	9.595E-01	1.062E+00
35	1.330E+00	1.057E+00	1.028E+00	9.957E-01	9.487E-01	1.055E+00	1.001E+00	9.487E-01	1.113E+00	9.602E-01	1.059E+00
36	1.335E+00	1.055E+00	1.027E+00	9.959E-01	9.500E-01	1.054E+00	1.001E+00	9.500E-01	1.110E+00	9.638E-01	1.057E+00
37	1.380E+00	1.054E+00	1.026E+00	9.963E-01	9.517E-01	1.052E+00	1.001E+00	9.517E-01	1.106E+00	9.649E-01	1.055E+00
38	1.420E+00	1.052E+00	1.026E+00	9.964E-01	9.523E-01	1.050E+00	1.001E+00	9.523E-01	1.104E+00	9.670E-01	1.054E+00
39	1.443E+00	1.048E+00	1.025E+00	9.964E-01	9.542E-01	1.047E+00	1.001E+00	9.542E-01	1.098E+00	9.668E-01	1.050E+00
40	1.465E+00	1.049E+00	1.025E+00	9.964E-01	9.534E-01	1.047E+00	1.001E+00	9.534E-01	1.099E+00	9.650E-01	1.051E+00
41	1.501E+00	1.048E+00	1.025E+00	9.964E-01	9.541E-01	1.047E+00	1.001E+00	9.541E-01	1.098E+00	9.652E-01	1.050E+00
42	1.533E+00	1.048E+00	1.025E+00	9.964E-01	9.544E-01	1.047E+00	1.001E+00	9.544E-01	1.098E+00	9.666E-01	1.050E+00

Sample 3. Continued

RUN NUMBER 83 PAGE 7

DATA TYPE 4
INTEGRAL EVALUATION

	ZP/DEL	PP/PPD	ML/MD	TTL/TTD	TL/TD	RHOL/RHOD	UL/UD	MUTL/MUTD	LRE/LRED	DITTL/DITTD	LRET/LRETD
43	1.569E+00	1.048E+00	1.024E+00	9.964E-01	9.560E-01	1.046E+00	1.001E+00	9.560E-01	1.095E+00	9.655E-01	1.050E+00
44	1.587E+00	1.047E+00	1.023E+00	9.964E-01	9.569E-01	1.046E+00	1.001E+00	9.569E-01	1.093E+00	9.652E-01	1.049E+00
45	1.632E+00	1.046E+00	1.023E+00	9.972E-01	9.580E-01	1.044E+00	1.001E+00	9.580E-01	1.091E+00	9.725E-01	1.047E+00
46	1.663E+00	1.044E+00	1.022E+00	9.973E-01	9.593E-01	1.042E+00	1.001E+00	9.593E-01	1.087E+00	9.709E-01	1.045E+00

M = 7.93
ALPHA = 0.0 DEG

PHI = 0.01
RS = 4.247E+00

DEL = 1.630E-01 IN
DEL* = 1.158E-01 IN
DEL** = 4.760E-03 IN

LRED = 1.363E+05 PER IN

VALUES AT DELTA

PPD = 4.920E+00 PSIA
MD = 6.1056E+00
TD = 1.554E+02 DEG R
TTD = 1.314E+03 DEG R
UD = 3.731E+03 FT/SEC

RHOD = 1.763E-03 LBM/FT3
RHOUD = 6.579E+00 LBM/SEC-FT2
MUTD = 1.251E-07 LBF-SEC/FT2
DITTD = 4.284E+01 BTU/LBM
LRETD = 2.384E+04 PER IN

Sample 3. Concluded

DATE COMPUTED 8-MAY-90
DATE RECORDED 8-MAY-90
TIME RECORDED 3:58: 25
TIME COMPUTED 03:58:54
PROJECT NUMBER CP91VB

HYPERSONIC BOUNDARY LAYER STABILITY

RUN NUMBER 28 PAGE 1

CONFIG: PRESSURE GRADIENT DP/DX: 4 (RN = 0.002 IN.)
XSTA = 15.00 IN.

DATA TYPE 2
MODEL SURFACE MEASUREMENTS

TAP	X (IN)	THETA (DEG)	PW (PSIA)	PW/P
1	12.0	180	0.0670	2.7755
2	14.0	180	0.0693	2.8736
3	16.0	180	0.0658	2.7269
4	18.0	180	0.0682	2.8273
5	22.0	180	0.0713	2.9551
6	23.0	180	0.0759	3.1467
7	24.0	180	0.0799	3.3111
8	25.0	180	0.0812	3.3645
9	26.0	180	0.0831	3.4457
10	27.0	180	0.0867	3.5942
11	28.0	180	0.0911	3.7761
12	29.0	180	0.0931	3.8588
13	30.0	180	0.0981	4.0671
14	31.0	180	0.0990	4.1011
15	32.0	180	0.0996	4.1275
16	33.0	180	0.1008	4.1789
17	34.0	180	0.1070	4.4323
18	35.0	180	0.1091	4.5227
19	36.0	180	0.1148	4.7592
20	37.0	180	0.1152	4.7753
21	38.0	180	0.1195	4.9512
22	38.0	270	0.1172	4.8588
23	38.0	0	0.1203	4.9863
24	38.0	90	0.1184	4.9084

T/C	X (IN)	THETA (DEG)	TW (DEG R)	TW/TT
1	12.00	90.00	884.2	0.674
2	14.00	90.00	799.4	0.609
3	16.00	90.00	777.5	0.593
4	18.00	90.00	745.6	0.568
5	22.00	90.00	774.3	0.590
6	23.00	90.00	790.9	0.603
7	24.00	90.00	807.9	0.616
8	25.00	90.00	834.5	0.636
9	26.00	90.00	858.5	0.655
10	27.00	90.00	885.6	0.675
11	28.00	90.00	911.9	0.695
12	29.00	90.00	929.4	0.709
13	30.00	90.00	942.5	0.719
14	31.00	90.00	942.9	0.719
15	32.00	90.00	945.3	0.721
16	33.00	90.00	938.9	0.716
17	34.00	90.00	935.1	0.713
18	35.00	90.00	930.5	0.709
19	36.00	90.00	920.0	0.701
20	37.00	90.00	894.0	0.682
21	36.00	95.75	917.3	0.699
22	36.00	101.50	920.3	0.702
23	36.35	102.10	910.2	0.694
24	36.70	102.70	901.5	0.687
25	37.05	103.30	890.0	0.679
26	37.40	103.90	873.3	0.666
27	37.75	104.50	852.4	0.650

ALPHA = 0.0 DEG
PHI = 0.0 DEG

XC = 15.931

PT = 225.5 PSIA
TT = 1311.7 DEG R
M = 7.933
RE = 0.100E+07 /FT

TDRK = 602.7 DEG R
P = 0.0241 PSIA
T = 98.4169 DEG R

RUN 28

Sample 4. Model Surface Measurements

HYPERSONIC BOUNDARY LAYER STABILITY
PROJECT NUMBER CP91VB

RUN NUMBER 4

DATA TYPE: SURFACE HEAT TRANSFER

DATE COMPUTED: 8-MAY-90
TIME COMPUTED: 01:57:02
DATE RECORDED: 8-MAY-90
TIME RECORDED: 1:56:23
000000135

PAGE 1

CONFIG: PRESSURE GRADIENT DP/DX: 4

GAGE	X, IN	THETA DEG	QDOT BTU/FT2-SEC	TW DEG R	HT(TT) BTU/FT2-SEC-R	ST(TT)
1	12.00	90.00				
2	14.00	90.00	0.687	555.86	9.155E-04	7.340E-04
3	16.00	90.00	0.587	556.15	7.818E-04	6.268E-04
4	18.00	90.00	0.618	552.70	8.202E-04	6.577E-04
5	22.00	90.00	0.952	588.42	1.325E-03	1.060E-03
6	23.00	90.00	1.176	575.83	1.609E-03	1.288E-03
7	24.00	90.00	1.438	582.56	1.986E-03	1.590E-03
8	25.00	90.00	1.473	583.75	2.037E-03	1.631E-03
9	26.00	90.00	1.504	587.44	2.090E-03	1.673E-03
10	27.00	90.00	1.774	590.98	2.478E-03	1.983E-03
11	28.00	90.00	1.672	591.02	2.336E-03	1.869E-03
12	29.00	90.00	1.729	591.22	2.417E-03	1.934E-03
13	30.00	90.00	2.051	595.94	2.885E-03	2.308E-03
14	31.00	90.00	1.671	591.19	2.336E-03	1.869E-03
15	32.00	90.00	1.715	592.64	2.402E-03	1.922E-03
16	33.00	90.00	1.651	590.48	2.305E-03	1.844E-03
17	34.00	90.00	1.677	590.37	2.342E-03	1.874E-03
18	35.00	90.00	1.621	589.02	2.259E-03	1.808E-03
19	36.00	90.00	1.797	589.19	2.505E-03	2.004E-03
20	37.00	90.00	1.700	586.04	2.359E-03	1.889E-03
21	36.00	95.75	1.659	589.15	2.312E-03	1.851E-03
22	36.00	101.50	1.750	590.34	2.443E-03	1.955E-03
23	36.35	102.10	1.828	588.09	2.544E-03	2.036E-03
24	36.70	102.70	1.640	586.98	2.279E-03	1.824E-03
25	37.05	103.30	1.865	[illegible]34.94	2.584E-03	2.068E-03
26	37.40	103.90	1.601	[illegible]0.80	2.206E-03	1.766E-03
27	37.75	104.50	1.715	576.04	2.347E-03	1.879E-03

PHI =	0.00	PT =	450.32 PSIA	V =	3853.83 FT/SEC
M =	7.98	TT =	1306.67 DEG R	Q =	2.09 PSIA
ALPHA =	-0.01 DEG	P =	0.05 PSIA	T =	97.15 DEG R
DEW =	-844.00 DEG F	RE =	1.994E+06 PER FT	PT2 =	3.87 PSIA
		MU =	7.818E-08 LBF-SEC/FT2	RHO =	1.302E-03 LBM/FT3

Sample 5. Model Surface Heat-Transfer Data